

Inference for a Large Directed Graphical Model with Interventions

Chunlin Li

School of Statistics, University of Minnesota, Minneapolis, MN 55455, USA

LI000007@UMN.EDU

Xiaotong Shen

School of Statistics, University of Minnesota, Minneapolis, MN 55455, USA

XSHEN@UMN.EDU

Wei Pan

Division of Biostatistics, University of Minnesota, Minneapolis, MN 55455, USA

PANXX014@UMN.EDU

Abstract

Inference of directed relations given some unspecified interventions, that is, the target of each intervention is not known, is important yet challenging. For instance, it is of high interest to unravel the regulatory roles of genes with inherited genetic variants like single-nucleotide polymorphisms (SNPs), which can be unspecified interventions because of their regulatory function on some unknown genes. In this article, we test hypothesized directed relations with unspecified interventions. First, we derive conditions to yield an identifiable model. Unlike classical inference, hypothesis testing requires identifying ancestral relations and relevant interventions for each hypothesis-specific primary variable, referring to as causal discovery. Towards this end, we propose a peeling algorithm to establish a hierarchy of primary variables as nodes, starting with leaf nodes at the hierarchy's bottom, for which we derive a difference-of-convex (DC) algorithm for nonconvex minimization. Moreover, we prove that the peeling algorithm yields consistent causal discovery, and the DC algorithm is a low-order polynomial algorithm capable of finding a global minimizer almost surely under the data generating distribution. Second, we propose a modified likelihood ratio test, eliminating nuisance parameters to increase power. To enhance finite-sample performance, we integrate the modified likelihood ratio test with a data perturbation scheme by accounting for the uncertainty of identifying ancestral relations and relevant interventions. Also, we show that the distribution of a data-perturbation test statistic converges to the target distribution in high dimensions. Numerical examples demonstrate the utility and effectiveness of the proposed methods, including an application to infer gene regulatory networks.

Keywords: High-dimensional inference, data perturbation, global nonconvex minimization, identifiability, testability, gene regulatory networks

1. Introduction

Directed (causal) relations are essential to explaining pairwise dependencies among multiple interacting units. In gene network analysis, regulatory gene-to-gene relations are a focus of biological investigation (Sachs et al., 2005), while, in a human brain network, scientists investigate causal influences among regions of interest to understand how the brain functions through the regional effects of neurons in terms of interregional connectivity (Liu et al., 2017). In such a situation, inferring directed effects without other information is generally impossible because of the issue of lack of identifiability as in a directed Gaussian graphical model without the strong equal-variance assumption (Peters and Bühlmann, 2014), and

hence external interventions are useful to treat a non-identifiable situation (Heinze-Deml et al., 2018). For instance, the regulatory roles of genetic variants such as single-nucleotide polymorphisms (SNPs) can help infer directed relations when treated as instrumental variables, where offspring randomly inherit alleles of SNPs from parents (Teumer, 2018; Molstad et al., 2021). This approach, similar to the randomized treatment assignment, is called Mendelian randomization. However, the targets (e.g. genes) of some regulatory SNPs (as instrumental variables) are unknown. Consequently, inferring directed relations (e.g. genes) while identifying relevant interventions (e.g. SNPs regulating the genes) for inference is critical. This paper focuses on the simultaneous inference of directed relations subject to unspecified interventions (i.e. without known targets) in a high-dimensional situation.

In a directed acyclic graph (DAG) model, the research has been centered on the reconstruction of directed relations in observational and interventional studies (Heinze-Deml et al., 2018; Zheng et al., 2018; Chickering, 2003; van de Geer and Bühlmann, 2013; Yuan et al., 2019; Oates et al., 2016; Aragam et al., 2019; Zhou et al., 2021). For inference, Bayesian methods (Friedman and Koller, 2003; Luo and Zhao, 2011; Viinikka et al., 2020) have been popular. Yet, statistical inference remains under-studied, especially for intervention models in high dimensions (Peters et al., 2016; Rothenhäusler et al., 2019). Recently, for observational data, Janková and van de Geer (2018) propose debiased tests for testing the strength of a directed linkage and Li et al. (2019) derives a constrained likelihood ratio test for multiple directed relations.

Despite progress, challenges remain. First, a formal inference requires identifying relevant interventions to yield an identifiable model. Besides, the concept of testability in Definition 2 is critical to hypothesis testing because directed relations, defined by the local Markov property (Spirtes et al., 2000), are subject to the acyclicity constraint (Yuan et al., 2019). As illustrated by Example 1, some hypotheses are not testable. Second, the standard debiasing treatment applies to testing the strength of a directed linkage given a known direction, ignoring the uncertainty of identifying the causal order (Janková and van de Geer, 2018). For interventional data, there lacks an inferential theory, especially in the presence of unspecified interventions. Third, one may need to deal with the super-exponentially many candidate relations.

To address the above issues, we develop modified likelihood ratio tests based on a data perturbation (DP) scheme, called a DP modified likelihood ratio test (DP-MLR), for testing (1) multiple causal relations and (2) the presence of a directed pathway. Unlike classical inference, hypothesis testing requires identifying ancestral relations and relevant interventions for each hypothesis-specific primary variable, referring to as causal discovery. Then, we propose a peeling algorithm to identify ancestral relations and relevant interventions, where we derive a difference-of-convex (DC) algorithm to treat nonconvex minimization. Note that the DP scheme is designed for the modified likelihood ratio tests to account for the identification uncertainty for the ancestral relations and relevant interventions. In particular, we establish four main results. First, a modified likelihood ratio test eliminates nuisance parameters for higher power, which is integrated with the DP scheme for more accurate finite-sample inference. Second, we derive conditions under which unspecified interventions yield model identifiability (Proposition 1) in a Gaussian directed graphical model. Also, we provide non-identifiable examples when the conditions break down. Third, we propose constrained L_0 -regressions subject to certain constraints (Proposition 2) to identify ancestral

relations and relevant interventions, which is integrated with a peeling algorithm (Algorithm 3) yielding consistent causal discovery (Theorem 3). To solve nonconvex minimization in a constrained regression, we develop a difference-of-convex (DC) algorithm (Algorithm 2) to solve a sequence of convex subproblems. Also, we show that it is in low-order polynomial time while yielding a *global* minimum almost surely in the data generating distribution (Theorem 3). Fourth, we provide a theoretical justification that the null distributions of DP-MLR converge to the target distributions (Theorem 4) under a weaker dimension restriction than that of the standard likelihood ratio test (Li et al., 2019) for an observational study. Moreover, our power analysis suggests that the proposed tests achieve the desired objective for inference (Propositions 6 and 7). To our knowledge, these results are the first in the literature, providing tools for testing multiple directed relations for unspecified interventions. Three attributing elements of these results are data perturbation, the peeling algorithm, and the modified likelihood ratio test.

The rest of the article is structured as follows. Section 2 establishes conditions for unspecified interventions to yield an identifiable model and introduces the notion of testability. Section 3 proposes our DP-MLR based on the ancestral relations and relevant interventions, estimated from constrained regressions. Moreover, we approximate the empirical null distribution of the proposed method by a DP method. Section 3 also develops a DC algorithm for constrained regressions, which guarantees a global minimizer almost surely. Section 4 is devoted to the theoretical justification of the proposed tests and power analysis. Section 5 performs simulations to compare the proposed test with the ideal oracle test, which uses the likelihood ratio test as if the graph structure were available in advance. Immediately after, we present an application to infer gene pathways with gene expression and SNP data. Finally, Section 7 concludes the article, followed by illustrative examples and technical proofs in the Appendix.

2. Directed Gaussian graphical models with interventions

To infer directed relations among primary variables $\mathbf{Y} = (Y_1, \dots, Y_p)^\top$, consider a structural equation model (Pearl, 2000) with interventions:

$$\mathbf{Y} = \mathbf{U}^\top \mathbf{Y} + \mathbf{W}^\top \mathbf{X} + \boldsymbol{\varepsilon}, \quad \boldsymbol{\varepsilon} \sim N(\mathbf{0}, \boldsymbol{\Sigma}), \quad \boldsymbol{\Sigma} = \text{Diag}(\sigma_1^2, \dots, \sigma_p^2), \quad (1)$$

where $\mathbf{X} = (X_1, \dots, X_q)^\top$ is a vector of intervention variables (observed exogenous variables representing interventions), $\mathbf{U} = (U_{kj})_{p \times p}$ and $\mathbf{W} = (W_{lj})_{q \times p}$ are unknown coefficient matrices, and $\boldsymbol{\varepsilon} = (\varepsilon_1, \dots, \varepsilon_p)^\top$ is a vector of random errors with $\sigma_j^2 > 0$; $j = 1, \dots, p$. In (1), $\boldsymbol{\varepsilon}$ is independent of \mathbf{X} but components of \mathbf{X} can be dependent. The matrix \mathbf{U} specifies the directed relations among \mathbf{Y} , where $U_{kj} \neq 0$ if Y_k is a direct cause of Y_j , denoted by $Y_k \rightarrow Y_j$. Thus, \mathbf{U} represents a directed graph, which is required to be acyclic to ensure the validity of the local Markov property (Spirtes et al., 2000). The matrix \mathbf{W} specifies the targets and strengths of interventions, where $W_{lj} \neq 0$ indicates X_l intervenes Y_j , denoted by $X_l \rightarrow Y_j$. In (1), no directed link from a primary variable Y_j to an intervention variable X_l is permissible. In other words, \mathbf{X} are non-descendants of \mathbf{Y} (Spirtes et al., 2000; Pearl, 2000).

In (1), $Y_k \rightarrow Y_j$ represents a parent-child relation, where Y_k is a parent of Y_j ; $k \neq j$. Moreover, this relation becomes an *immediate parent-child relation* denoted by $Y_k \Rightarrow Y_j$

if there does not exist another directed pathway connecting them, where Y_k is called an *immediate parent* of Y_j . Finally, $Y_k \rightsquigarrow Y_j$ represents an ancestral relation if there exists a directed pathway connecting them, that is, $Y_k = Y_{k_0} \rightarrow Y_{k_1} \rightarrow \dots \rightarrow Y_{k_\nu} = Y_j$, where Y_k is an ancestor of Y_j . Note that a parent is also an ancestor by this definition. See Figure 1 for illustration.

2.1 Identifiability

Model (1) is generally non-identifiable without interventions ($\mathbf{W} = \mathbf{0}$) when the equal-variance assumption ($\sigma_1^2 = \dots = \sigma_p^2$) does not hold (Peters and Bühlmann, 2014). Moreover, a model can be identified when ε in (1) is replaced by non-Gaussian errors (Shimizu et al., 2006) or linear relations are replaced by nonlinear ones (Hoyer et al., 2009). Regardless, suitable interventions can make (1) identifiable, as to be seen in Proposition 1. It is worth noting that when intervention targets are known (Pearl, 2000), the identifiability issue has been extensively studied (Oates et al., 2016; Chen et al., 2018). However, it is less so when the exact targets and strengths of interventions are unknown, as in many biological applications (Jackson et al., 2003; Kulkarni et al., 2006), referring to the case of *unspecified* or *uncertain* interventions (Heinze-Deml et al., 2018; Eaton and Murphy, 2007; Squires et al., 2020).

We now categorize interventions as instruments and noninstruments (covariates).

Definition 1 (Instrument) *An intervention is an instrument if it satisfies:*

- (A) *Relevance: it intervenes on at least one primary variable;*
- (B) *Exclusion: it does not intervene on more than one primary variable.*

In short, instruments are essential to discovering directed relations, as suggested by Proposition 2, whereas noninstruments do not satisfy (A) or (B) in Definition 1. Here, (A) requires an intervention to be active, while (B) prevents simultaneous interventions of a single intervention variable on multiple primary variables. That is critical to causal discovery because an intervention on a cause variable Y_1 helps reveal its causal effect on an outcome variable Y_2 , which would otherwise be impossible. Thus, the instruments are useful to break the symmetry that results in non-identifiability of directed relations $Y_1 \rightarrow Y_2$ and $Y_2 \rightarrow Y_1$.

Next, we make some assumptions on intervention variables to yield an identifiable model, where dependencies among intervention variables are permissible, which is particularly suited for dependent SNPs in gene regulatory network analysis.

Assumption 1 *Assume that model (1) satisfies the following conditions.*

- (1A) *(Non-degeneracy) $E \mathbf{X} \mathbf{X}^\top$ is positive definite, where E denotes the expectation.*
- (1B) *(Local faithfulness) $\text{Cov}(Y_j, X_l \mid \mathbf{X}_{\{1, \dots, q\} \setminus \{l\}}) \neq 0$ when X_l intervenes on an immediate parent of Y_j , where Cov is the covariance.*
- (1C) *(Relevance and exclusion) Each primary variable is intervened by at least one instrument.*

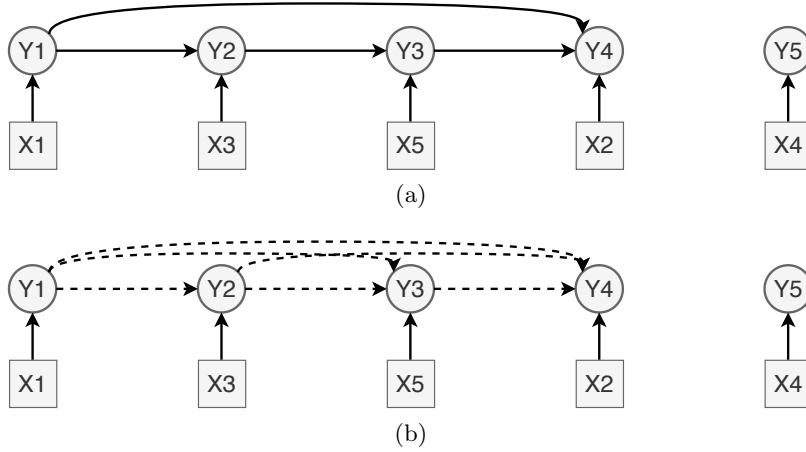


Figure 1: (a) A true DAG structure of five primary variables Y_1, \dots, Y_5 and five intervention variables X_1, \dots, X_5 , where directed edges are represented by solid arrows while dependencies among \mathbf{X} are not display. Note that \mathcal{A} contains six ancestral relations $Y_1 \Rightarrow Y_2$, $Y_2 \Rightarrow Y_3$, $Y_3 \Rightarrow Y_4$, $Y_1 \rightsquigarrow Y_4$, $Y_1 \rightsquigarrow Y_3$, and $Y_2 \rightsquigarrow Y_4$. Note that Y_1 is a parent of Y_4 but not an immediate parent of Y_4 . (b) In the same graph, dashed arrows display six estimated ancestral relations of primary variables by Algorithm 3 in Example 3, $Y_1 \Rightarrow Y_2$, $Y_2 \Rightarrow Y_3$, $Y_3 \Rightarrow Y_4$, $Y_1 \rightsquigarrow Y_4$, $Y_1 \rightsquigarrow Y_3$, and $Y_2 \rightsquigarrow Y_4$.

Assumption 1 imposes mild distributional restrictions on \mathbf{X} , permitting discrete variables such as SNPs. Importantly, if either Assumption 1B or Assumption 1C fails, model (1) is not identifiable, as shown in Example 2 of the Appendix. Assumption 1B requires interventional effects not to cancel out as multiple targets from a noninstrument are permitted. Note that Assumption 1B is generally mild but may break down, especially when some components of \mathbf{X} are deterministic functions of the others.

Proposition 1 (Identifiability) *Under Assumption 1, model (1) is identifiable.*

Proposition 1 is derived for unspecified interventions. It is in contrast to Proposition 1 of (Chen et al., 2018), which uses Assumption 1C to prove the identifiability with target-known instruments.

We remark that an intervention on an immediate parent is essential to identifying directed relations because of Assumption 1B. Therefore, we call X_l a *relevant intervention* of Y_j , denoted by $X_l \Rightarrow Y_j$, if X_l intervenes on Y_j ($X_l \rightarrow Y_j$) or an immediate parent of Y_j ($X_l \rightarrow Y_k \Rightarrow Y_j$).

2.2 Testability

Our primary goal is to perform a hypothesis test, which requires identifying relevant interventions for inference. To this end, let $F \subseteq \{1, \dots, p\}^2$ be an edge set, where $(k, j) \in F$ specifies a directed link $Y_k \rightarrow Y_j$ in (1). We shall focus on two types of testing with null and alternative hypotheses H_0 and H_a , motivated from gene network analysis. For simultaneous testing of directed linkages,

$$H_0 : U_{kj} = 0; \text{ for all } (k, j) \in F \quad \text{versus} \quad H_a : U_{kj} \neq 0 \text{ for some } (k, j) \in F; \quad (2)$$

for simultaneous testing of pathways,

$$H_0 : U_{kj} = 0; \text{ for some } (k, j) \in F \quad \text{versus} \quad H_a : U_{kj} \neq 0 \text{ for all } (k, j) \in F, \quad (3)$$

where $((U_{kj})_{(k,j) \in F^c}, \mathbf{W}, \mathbf{\Sigma})$ are unspecified nuisance parameters and c is the set complement.

In (2) and (3), due to the acyclicity constraint, some links are absent in the true model, which makes an inference under (1) dramatically different from other statistical models. Formally, we define the concept of testability of H_0 .

Definition 2 (Testability)

- (A) A link $(k, j) \in F$ is testable if $\{(k, j)\} \cup E$ forms a DAG, where E denotes the index set of nonzero elements of the adjacency matrix \mathbf{U} in (1).
- (B) Let $D \subseteq F$ be a set of all testable links under H_0 , where $D \cup E$ forms a DAG. Then H_0 is testable with respect to \mathbf{U} if $D \neq \emptyset$.

Example 1 Consider the DAG displayed in Figure 1. By Definition 2, $H_0 : U_{21} = 0$ is not testable with $D = \emptyset$ since $Y_1 \rightarrow Y_2 \rightarrow Y_1$ forms a directed cycle under H_0 . Hence the parameter space under H_a is identical to that under H_0 with respect to the true model. Now consider $H_0 : U_{45} = U_{53} = 0$. Then $F = D = \{(4, 5), (5, 3)\}$, but this is again not testable because $Y_3 \rightarrow Y_4 \rightarrow Y_5 \rightarrow Y_3$ gives a directed cycle.

The above discussion suggests that testability is essential for the likelihood ratio test. In practice, D needs to be estimated from data; see Algorithm 3. Throughout this article, although we focus on testable hypotheses, we define the p-value of a hypothesis testing to be one in a non-testable case.

3. Likelihood inference

This section develops simultaneous tests of directed linkages (2) and pathways (3). Given an independent and identically distributed sample $(\mathbf{Y}_i, \mathbf{X}_i)_{i=1}^n$ from (1), the log-likelihood is written as (up to additive constant)

$$l(\boldsymbol{\theta}) = -\frac{1}{2} \sum_{i=1}^n ((\mathbf{I} - \mathbf{U}^\top) \mathbf{Y}_i - \mathbf{W}^\top \mathbf{X}_i)^\top \mathbf{\Sigma}^{-1} ((\mathbf{I} - \mathbf{U}^\top) \mathbf{Y}_i - \mathbf{W}^\top \mathbf{X}_i) - n \log \sqrt{\det(\mathbf{\Sigma})}, \quad (4)$$

where \mathbf{U} is subject to the acyclicity constraint that no directed loops are permissible for \mathbf{U} to induce a DAG (Yuan et al., 2019).

Let $\text{AN}(j) = \{k : Y_k \rightsquigarrow Y_j\}$ and $\text{INT}(j) = \{l : X_l \Rightarrow Y_j\}$ be the ancestor and relevant intervention index sets of Y_j , respectively. Let $\mathcal{A} = \{(k, j) : Y_k \rightsquigarrow Y_j\}$ be the set of all ancestral relations, and $\mathcal{I} = \{(l, j) : X_l \Rightarrow Y_j\}$ be a set of all relevant intervention relations.

For simplicity, we reparametrize $\boldsymbol{\theta}$ in (4) by focusing on nonzero elements of \mathbf{U} and \mathbf{W} , defined by $\mathcal{S} = (\mathcal{A}, \mathcal{I})$ encoding all ancestral relations and relevant interventions. Let $\boldsymbol{\theta}_{\mathcal{S}}$ be

$((U_{kj})_{(k,j) \in \mathcal{A}}, (W_{lj})_{(l,j) \in \mathcal{I}})$ to represent $\boldsymbol{\theta}$ restricted to \mathcal{S} . Then, $l(\boldsymbol{\theta})$ in (4) can be rewritten by removing zero elements of \mathbf{U} and \mathbf{W} ,

$$\begin{aligned} l(\boldsymbol{\theta}_{\mathcal{S}}, \boldsymbol{\Sigma}) &= - \sum_{j=1}^p \left(\text{RSS}_j(\boldsymbol{\theta}_{\mathcal{S}}) / 2\sigma_j^2 + \log \sqrt{2\pi\sigma_j^2} \right), \\ \text{RSS}_j(\boldsymbol{\theta}_{\mathcal{S}}) &= \sum_{i=1}^n \left(Y_{ij} - \sum_{(k,j) \in \mathcal{A}} U_{kj} Y_{ik} - \sum_{(l,j) \in \mathcal{I}} W_{lj} X_{il} \right)^2, \end{aligned} \quad (5)$$

which involves $(|\mathcal{A}| + |\mathcal{I}| + p)$ parameters for $\boldsymbol{\theta}_{\mathcal{S}}$. Given $(\mathcal{S}, \boldsymbol{\Sigma})$, $l(\boldsymbol{\theta}_{\mathcal{S}}, \boldsymbol{\Sigma})$ is convex in $\boldsymbol{\theta}_{\mathcal{S}}$. In contrast, a full likelihood approach aims to optimize over $(\boldsymbol{\theta}_{\mathcal{S}}, \mathcal{S}, \boldsymbol{\Sigma})$, where \mathcal{S} has super-exponentially many configurations.

3.1 Modified likelihood ratio test via data perturbation

To achieve high power while controlling the Type I error, we propose a modified likelihood ratio statistic given an estimate $(\hat{\mathcal{S}}, \hat{\boldsymbol{\Sigma}})$ of $(\mathcal{S}, \boldsymbol{\Sigma})$, which separates the inference of continuous parameters $\boldsymbol{\theta}_{\mathcal{S}}$ from the estimation of high-dimensional categorical parameter \mathcal{S} and nuisance parameter $\boldsymbol{\Sigma}$, while eliminating many irrelevant nuisance parameters. Here $\hat{\boldsymbol{\Sigma}}$ is given in (7) and $\hat{\mathcal{S}}$ is obtained in Section 3.2.

First, we construct a likelihood ratio $\text{Lr}(\mathcal{S}, \boldsymbol{\Sigma})$ in (6) and then plug-in an estimate $(\hat{\mathcal{S}}, \hat{\boldsymbol{\Sigma}})$. Then we perform a likelihood ratio test via data perturbation, accounting for the uncertainty of estimating \mathcal{S} .

MODIFIED LIKELIHOOD RATIO

Consider the test in (2). From (5), the likelihood ratio statistic is

$$\begin{aligned} \text{Lr}(\mathcal{S}, \boldsymbol{\Sigma}) &= l(\hat{\boldsymbol{\theta}}_{\mathcal{S}}^{(1)}, \boldsymbol{\Sigma}) - l(\hat{\boldsymbol{\theta}}_{\mathcal{S}}^{(0)}, \boldsymbol{\Sigma}) = \sum_{j=1}^p \left(\text{RSS}_j(\hat{\boldsymbol{\theta}}_{\mathcal{S}}^{(0)}) - \text{RSS}_j(\hat{\boldsymbol{\theta}}_{\mathcal{S}}^{(1)}) \right) / 2\sigma_j^2 \\ &= \sum_{\{j: \exists (k,j) \in D\}} \left(\text{RSS}_j(\hat{\boldsymbol{\theta}}_{\mathcal{S}}^{(0)}) - \text{RSS}_j(\hat{\boldsymbol{\theta}}_{\mathcal{S}}^{(1)}) \right) / 2\sigma_j^2, \end{aligned} \quad (6)$$

where $\hat{\boldsymbol{\theta}}_{\mathcal{S}}^{(0)} = \arg \max_{\boldsymbol{\theta}_{\mathcal{S}}} l(\boldsymbol{\theta}_{\mathcal{S}}, \boldsymbol{\Sigma})$ and $\hat{\boldsymbol{\theta}}_{\mathcal{S}}^{(1)} = \arg \max_{\boldsymbol{\theta}_{\mathcal{S}}} l(\boldsymbol{\theta}_{\mathcal{S}}, \boldsymbol{\Sigma})$ are the maximum likelihood estimates (MLE) given $(\mathcal{S}, \boldsymbol{\Sigma})$ under H_0 and H_a , D is the set of testable links of H_0 (Definition 2), and $\text{RSS}_{j^*}(\hat{\boldsymbol{\theta}}_{\mathcal{S}}^{(0)}) = \text{RSS}_{j^*}(\hat{\boldsymbol{\theta}}_{\mathcal{S}}^{(1)})$ for $j^* \notin \{j : \exists (k,j) \in D\}$, because no H_0 constraint is imposed for these primary variables. Hence, $\text{Lr}(\mathcal{S}, \boldsymbol{\Sigma})$ in (6) summarizes only the contributions from the ancestral relations of hypothesized primary variables under H_0 . Note that $\text{RSS}_j(\hat{\boldsymbol{\theta}}_{\mathcal{S}}^{(0)}) - \text{RSS}_j(\hat{\boldsymbol{\theta}}_{\mathcal{S}}^{(1)})$ depends only on parameters in the j th column of \mathbf{U} and \mathbf{W} in the j th structural equation of (1). Thus, a large number of nuisance parameters associated with $Y_j; \forall (k,j) \notin D$ are eliminated in (6).

The modified likelihood ratio becomes $\text{Lr} = \text{Lr}(\hat{\mathcal{S}}, \hat{\boldsymbol{\Sigma}})$, where we compute an estimate $\hat{\mathcal{S}}$ of \mathcal{S} from Algorithm 3 in Section 3.2 and obtain an $\hat{\boldsymbol{\Sigma}} = (\hat{\sigma}_1^2, \dots, \hat{\sigma}_p^2)^\top$ of $\boldsymbol{\Sigma}$:

$$\hat{\sigma}_j^2 = \text{RSS}_j \left(\hat{\boldsymbol{\theta}}_{\hat{\mathcal{S}}}^{(1)} \right) / \left(n - |\widehat{\text{AN}}(j)| - |\widehat{\text{INT}}(j)| \right); \quad j = 1, \dots, p, \quad (7)$$

where $\widehat{\text{AN}}(j)$ and $\widehat{\text{INT}}(j)$ are the estimated ancestor set and relevant intervention set of Y_j . An adjustment to the degrees of freedom yields an approximately unbiased estimator in that $E\hat{\sigma}_j^2 \approx \sigma_j^2$; $j = 1, \dots, p$, which reduces the bias particularly when $|\text{AN}(j)| + |\text{INT}(j)|$ is large.

The modified likelihood ratio in (6) requires the estimation of \mathcal{S} , where we must account for the uncertainty of identification for accurate finite-sample inference. To this end, consider any “correct” model $\mathcal{S} \supseteq \mathcal{S}^0$, where $\mathcal{S} = (\mathcal{A}, \mathcal{I}) \supseteq \mathcal{S}^0 = (\mathcal{A}^0, \mathcal{I}^0)$ means that $\text{AN}(j) \supseteq \text{AN}^0(j)$ and $\text{INT}(j) \supseteq \text{INT}^0(j)$ for j with $\exists(k, j) \in D$ and 0 denotes the truth. A “correct” model has no approximation error, yet may lead to inference with less power when \mathcal{S} is much larger than \mathcal{S}^0 . By comparison, an inference based on $\mathcal{S} \not\supseteq \mathcal{S}^0$ is biased, accompanied by an inflated Type I error.

TESTING DIRECTED LINKAGES (2) VIA DATA PERTURBATION

Let $\mathbb{Z} = (\mathbb{Y}, \mathbb{X}) \in \mathbb{R}^{n \times (p+q)}$, $\mathbb{Y} = (\mathbf{Y}_1, \dots, \mathbf{Y}_n)^\top \in \mathbb{R}^{n \times p}$, and $\mathbb{X} = (\mathbf{X}_1, \dots, \mathbf{X}_n)^\top \in \mathbb{R}^{n \times q}$. Let $\mathbf{e}_j \in \mathbb{R}^n$ be the j th column of $\mathbf{e} = (\boldsymbol{\varepsilon}_1, \dots, \boldsymbol{\varepsilon}_n)^\top \in \mathbb{R}^{n \times p}$. From (6), assuming over-identification $\widehat{\mathcal{S}} \supseteq \mathcal{S}^0$, we can write the likelihood ratio as

$$\begin{aligned} \text{Lr} &= \frac{1}{2} \sum_{j: \exists(k, j) \in \widehat{D}} \frac{\mathbb{Y}_j^\top (\mathbf{P}_{\widehat{A}_j} - \mathbf{P}_{\widehat{B}_j}) \mathbb{Y}_j}{\mathbb{Y}_j^\top (\mathbf{I} - \mathbf{P}_{\widehat{A}_j}) \mathbb{Y}_j / (n - |\widehat{A}_j|)} \\ &= \frac{1}{2} \sum_{j: \exists(k, j) \in \widehat{D}} \frac{(\mathbb{Y}_{\{k: (k, j) \in \widehat{D}\}} \mathbf{U}_{\{k: (k, j) \in \widehat{D}\}} + \mathbf{e}_j)^\top (\mathbf{P}_{\widehat{A}_j} - \mathbf{P}_{\widehat{B}_j}) (\mathbb{Y}_{\{k: (k, j) \in \widehat{D}\}} \mathbf{U}_{\{k: (k, j) \in \widehat{D}\}} + \mathbf{e}_j)}{\mathbf{e}_j^\top (\mathbf{I} - \mathbf{P}_{\widehat{A}_j}) \mathbf{e}_j / (n - |\widehat{A}_j|)}, \end{aligned} \quad (8)$$

where $\mathbf{P}_A = \mathbb{Z}_A (\mathbb{Z}_A^\top \mathbb{Z}_A)^{-1} \mathbb{Z}_A^\top$ is the projection matrix onto the span of columns A in \mathbb{Z} , $\widehat{A}_j = \widehat{\text{AN}}(j) \cup \widehat{\text{INT}}(j)$, $\widehat{B}_j = \widehat{A}_j \setminus \{k : (k, j) \in D\} \subseteq \widehat{A}_j$, and the second equality in (8) follows from (1). Note that under H_0 , $\mathbf{U}_{\{k: (k, j) \in D\}} = \mathbf{0}$ for all j , while under H_a , $\mathbf{U}_{\{k: (k, j) \in D\}} \neq \mathbf{0}$ for some j .

We propose a data perturbation (DP) method (Shen and Ye, 2002) to approximate the null distribution of Lr in (8). The idea behind DP is to assess the sensitivity of the estimates through perturbed data $\mathbf{Y}_i^* = \mathbf{Y}_i + \boldsymbol{\varepsilon}_i^*$, where $\boldsymbol{\varepsilon}_i^* \sim N(0, \delta^2 \widehat{\boldsymbol{\Sigma}})$ and $0 < \delta \leq 1$ is the perturbation size; $i = 1, \dots, n$. DP may trace back to the little bootstrap (Breiman, 1992). Now, we develop a DP method for inference to account for the uncertainty of identifying ancestors and relevant interventions.

Let $\mathcal{Z}^* = (\mathbf{X}_i, \mathbf{Y}_i^*, \boldsymbol{\varepsilon}_i^*)_{i=1}^n$ be a perturbed sample, with $\mathbf{e}^* = (\mathbf{e}_1^*, \dots, \mathbf{e}_p^*) = (\boldsymbol{\varepsilon}_1^*, \dots, \boldsymbol{\varepsilon}_n^*)^\top \in \mathbb{R}^{n \times p}$ denoting perturbation errors. Given \mathcal{Z}^* , we obtain a perturbation estimate $\widehat{\mathcal{S}}^*$. Assume over-selection in that $\widehat{\mathcal{S}}^* \supseteq \mathcal{S}^0$, a naive DP likelihood ratio $\text{Lr}(\widehat{\mathcal{S}}^*, \widehat{\boldsymbol{\Sigma}}^*)$ based on \mathcal{Z}^* is

$$\frac{1}{2} \sum_{j: \exists(k, j) \in \widehat{D}} \frac{(\mathbb{Y}_{\{k: (k, j) \in D\}} \mathbf{U}_{\{k: (k, j) \in D\}} + \mathbf{e}_j^* + \mathbf{e}_j)^\top (\mathbf{P}_{\widehat{A}_j^*} - \mathbf{P}_{\widehat{B}_j^*}) (\mathbb{Y}_{\{k: (k, j) \in D\}} \mathbf{U}_{\{k: (k, j) \in D\}} + \mathbf{e}_j^* + \mathbf{e}_j)}{(\mathbf{e}_j^* + \mathbf{e}_j)^\top (\mathbf{I} - \mathbf{P}_{\widehat{A}_j^*}) (\mathbf{e}_j^* + \mathbf{e}_j) / (n - |\widehat{A}_j^*|)}.$$

Note that the errors \mathbf{e}_j given $(\mathbf{X}_i, \mathbf{Y}_i)_{i=1}^n$ is deterministic and does not vanish under either H_0 or H_a . Thus, the conditional distribution of $\text{Lr}(\widehat{\mathcal{S}}^*, \widehat{\boldsymbol{\Sigma}}^*)$ given $(\mathbf{X}_i, \mathbf{Y}_i)_{i=1}^n$ does not approximate the null distribution of Lr in (8).

To overcome this difficulty, we introduce our DP test statistic Lr^* . In (8), under H_0 , $\text{Lr} = f(\mathbb{X}, \boldsymbol{\mu}, \mathbf{e})$ is a function of intervention data \mathbb{X} , conditional mean $\boldsymbol{\mu} = (\mathbb{E}(\mathbf{Y}_1 | \mathbf{X}_1), \dots, \mathbb{E}(\mathbf{Y}_n | \mathbf{X}_n))^\top \in \mathbb{R}^{n \times p}$ and unobserved error \mathbf{e} , where $\mathbb{E}(\mathbf{Y}_i | \mathbf{X}_i) = (\mathbb{E}(Y_{i1} | \mathbf{X}_i), \dots, \mathbb{E}(Y_{ip} | \mathbf{X}_i))^\top \in \mathbb{R}^p$; $i = 1, \dots, n$. However, the perturbation error \mathbf{e}^* is *known* given the DP sample \mathcal{Z}^* , suggesting a form Lr^* based on Lr :

$$\text{Lr}^* \equiv f(\mathbb{X}, \mathbb{Y}, \mathbf{e}^*) = \frac{1}{2} \sum_{j: \exists (k,j) \in \widehat{D}} \frac{(\mathbf{e}_j^*)^\top (\mathbf{P}_{\widehat{A}_j^*} - \mathbf{P}_{\widehat{B}_j^*}) \mathbf{e}_j^*}{(\mathbf{e}_j^*)^\top (\mathbf{I} - \mathbf{P}_{\widehat{A}_j^*}) \mathbf{e}_j^* / (n - |\widehat{A}_j^*|)}, \quad (9)$$

which mimics (8) under H_0 , or $\mathbf{U}_{\{k:(k,j) \in D\}} = \mathbf{0}$, with \mathbf{e}_j replaced by \mathbf{e}_j^* . As a result, when $\widehat{\mathcal{S}}^* \supseteq \mathcal{S}^0$, the conditional distribution of Lr^* given $(\mathbf{X}_i, \mathbf{Y}_i)_{i=1}^n$ well approximates the null distribution of Lr , where the model selection effect is accounted for by assessing the variability of \widehat{A}_j^* over different realizations of \mathcal{Z}^* .

In practice, we use Monte-Carlo to approximate the distribution of Lr^* given $(\mathbf{X}_i, \mathbf{Y}_i)_{i=1}^n$ in (9). In particular, we generate M perturbed samples $(\mathcal{Z}_m^*)_{m=1}^M$ independently and compute Lr_m^* ; $m = 1, \dots, M$. Then, we examine the over-selection condition $\widehat{\mathcal{S}}_m^* \supseteq \mathcal{S}^0$ by checking its empirical counterpart $\widehat{\mathcal{S}}_m^* \supseteq \widehat{\mathcal{S}}$. The DP p-value of linkage test in (2) is defined as

$$\text{Pval} = \left(\sum_{m=1}^M \mathbb{I}(\text{Lr}_m^* \geq \text{Lr}, \widehat{\mathcal{S}}_m^* \supseteq \widehat{\mathcal{S}}) \right) / \left(\sum_{m=1}^M \mathbb{I}(\widehat{\mathcal{S}}_m^* \supseteq \widehat{\mathcal{S}}) \right), \quad (10)$$

where $\mathbb{I}(\cdot)$ is the indicator function.

EXTENSION TO HYPOTHESIS TESTING FOR PATHWAYS (3)

Next, we extend the DP inference for (3). Denote $F = \{(k_1, j_1), \dots, (k_{|F|}, j_{|F|})\}$. Then the test of pathways in (3) can be reduced to testing sub-hypotheses

$$H_{0,\nu} : U_{k_\nu, j_\nu} = 0, \quad \text{versus} \quad H_{a,\nu} : U_{k_\nu, j_\nu} \neq 0; \quad \nu = 1, \dots, |F|,$$

where each sub-hypothesis is a linkage test. Given $(\mathcal{S}, \boldsymbol{\Sigma})$, the likelihood ratio for $H_{0,\nu}$ is $\text{Lr}_\nu(\mathcal{S}, \boldsymbol{\Sigma}) = l(\widehat{\boldsymbol{\theta}}_{\mathcal{S}}^{(1)}, \boldsymbol{\Sigma}) - l(\widehat{\boldsymbol{\theta}}_{\mathcal{S}}^{(0,\nu)}, \boldsymbol{\Sigma})$, where $\widehat{\boldsymbol{\theta}}_{\mathcal{S}}^{(0,\nu)}$ is the MLE under the constraint that $U_{k_\nu, j_\nu} = 0$. Then for $\widehat{\mathcal{S}} \supseteq \mathcal{S}^0$, we have

$$\begin{aligned} \text{Lr}_\nu &= \frac{1}{2} \frac{(\mathbb{Y}_{k_\nu} U_{k_\nu} + \mathbf{e}_{j_\nu})^\top (\mathbf{P}_{\widehat{A}_{j_\nu}} - \mathbf{P}_{\widehat{B}_{j_\nu}}) (\mathbb{Y}_{k_\nu} U_{k_\nu} + \mathbf{e}_{j_\nu})}{(\mathbf{e}_{j_\nu})^\top (\mathbf{I} - \mathbf{P}_{\widehat{A}_{j_\nu}}) \mathbf{e}_{j_\nu} / (n - |\widehat{A}_{j_\nu}|)}, \\ \text{Lr}_\nu^* &= \frac{1}{2} \frac{(\mathbf{e}_{j_\nu}^*)^\top (\mathbf{P}_{\widehat{A}_{j_\nu}^*} - \mathbf{P}_{\widehat{B}_{j_\nu}^*}) \mathbf{e}_{j_\nu}^*}{(\mathbf{e}_{j_\nu}^*)^\top (\mathbf{I} - \mathbf{P}_{\widehat{A}_{j_\nu}^*}) \mathbf{e}_{j_\nu}^* / (n - |\widehat{A}_{j_\nu}^*|)}, \end{aligned} \quad (11)$$

where the distributions of Lr_ν^* given $(\mathbf{X}_i, \mathbf{Y}_i)_{i=1}^n$ approximates the null distributions of Lr_ν . Finally, define the p-value of pathway test in (3) as

$$\text{Pval} = \max_{1 \leq \nu \leq |F|} \left(\sum_{m=1}^M \mathbb{I}(\text{Lr}_{\nu,m}^* \geq \text{Lr}_\nu, \widehat{\mathcal{S}}_m^* \supseteq \widehat{\mathcal{S}}) \right) / \left(\sum_{i=1}^M \mathbb{I}(\widehat{\mathcal{S}}_m^* \supseteq \widehat{\mathcal{S}}) \right). \quad (12)$$

Note that if any $H_{0,\nu}$ is not testable, then we have $\text{Pval} = 1$.

Algorithm 1 summarizes the DP method for hypothesis testing of (2) and (3).

Algorithm 1: Parallelizable algorithm for DP testing

- 1 Specify the size of Monte Carlo M . Apply Algorithm 3 to original data \mathcal{Z} to compute $\hat{\Sigma} = (\hat{\sigma}_1^2, \dots, \hat{\sigma}_p^2)^\top$ by (7).
 - 2 (**Parallelizable version**) Generate perturbed data $\mathcal{Z}_m^* = \{(\mathbf{X}_i, \mathbf{Y}_{m,i}^*, \boldsymbol{\epsilon}_{m,i}^*)_{i=1}^n\}$ in parallel, where $\boldsymbol{\epsilon}_{m,i}^* \sim N(\mathbf{0}, \delta^2 \hat{\Sigma})$. For (2), compute Lr_m^* based on \mathcal{Z}_m^* , while, for (3), compute $\text{Lr}_{\nu,m}^*$; $\nu = 1, \dots, |F|$ based on \mathcal{Z}_m^* ; $m = 1, \dots, M$.
 - 3 Compute the p-value of a test as (10) or (12) accordingly.
-

Remark 1 (Computation) *To accelerate the computation, we consider a parallelizable procedure in Algorithm 1. In addition, we use the original estimate $\hat{\boldsymbol{\theta}}$ as a warm-start initialization for the DP estimates, which effectively reduces the computing time.*

Remark 2 (Connection with bootstrap) *Ideally, one may consider parametric or non-parametric bootstrap for Lr , where parametric bootstrap requires a good initial estimate of some parameters. Yet, it is rather challenging to correct the bias of this estimate because of the acyclicity constraint. By comparison, DP does not rely on such an estimate, as shown in (9). On the other hand, nonparametric bootstrap resamples the original data with replacement. In a bootstrap sample, only about 63% distinct observations in the original data involve model selection and fitting, leading to deteriorating performance (Kleiner et al., 2012). As a result, nonparametric bootstrap may not well-approximate the distribution of Lr . In contrast, DP provides a better approximation of Lr via (9), taking advantage of a full sample. In this regard, DP is more suitable than bootstrap in our situation.*

3.2 Estimation of ancestral and interventional relations

This section develops a constrained regression method to estimate $\mathcal{S} = (\mathcal{A}, \mathcal{I})$ in (5). First, we observe an important connection between primary variables and intervention variables. Rewrite (1) as

$$\mathbf{Y} = \mathbf{V}^\top \mathbf{X} + \boldsymbol{\epsilon}_V, \quad \boldsymbol{\epsilon}_V = (\mathbf{I} - \mathbf{U}^\top)^{-1} \boldsymbol{\epsilon} \sim N(\mathbf{0}, \boldsymbol{\Omega}^{-1}), \quad (13)$$

where $\boldsymbol{\Omega} = (\mathbf{I} - \mathbf{U})\boldsymbol{\Sigma}^{-1}(\mathbf{I} - \mathbf{U}^\top)$ is a precision matrix and $\mathbf{V} = \mathbf{W}(\mathbf{I} - \mathbf{U})^{-1}$. Then $V_{lj} \neq 0$ implies the dependence of Y_j on X_l through the local Markov property defined by (1), and hence that X_l intervenes on Y_j or an ancestor of Y_j . Proposition 2 formalizes this statement.

Let $\mathbf{V}_{l\bullet} \in \mathbb{R}^p$ and $\mathbf{V}_{\bullet j} \in \mathbb{R}^q$ denote the l th row and j th column vectors of \mathbf{V} , respectively.

Proposition 2 (Identification of \mathcal{S} via \mathbf{V}) *Suppose Assumption 1 is satisfied.*

- (A) *If $V_{lj} \neq 0$, then X_l intervenes on Y_j or an ancestor of Y_j ;*
- (B) *Y_j is a leaf variable (having no children) iff there exists an instrument X_l such that $V_{lj} \neq 0$ and $\|\mathbf{V}_{l\bullet}\|_0 = 1$; $l = 1, \dots, q$.*
- (C) *If $V_{lj} \neq 0$ and X_l is an instrument variable for Y_k , then $Y_k \rightsquigarrow Y_j$ encodes an ancestral relation.*

Next we use L_0 -constrained linear regressions to estimate nonzero elements of \mathbf{V} in (13) column by column:

$$\hat{\mathbf{V}}_{\bullet j} = \arg \min_{\mathbf{V}_{\bullet j}} (2n)^{-1} \sum_{i=1}^n (Y_{ij} - \mathbf{V}_{\bullet j}^\top \mathbf{X}_i)^2 \quad \text{s.t.} \quad \sum_{l=1}^q \mathbf{I}(V_{lj} \neq 0) \leq K_j; \quad j = 1, \dots, p, \quad (14)$$

where $1 \leq K_j \leq q$ is an integer-valued tuning parameter controlling the sparsity of the solution, and can be chosen by cross-validation; see Section 5.

To solve (14), we use $J_{\tau_j}(z) = \min(|z|/\tau_j, 1)$ as a surrogate of the L_0 -function $\mathbf{I}(z \neq 0)$ (Shen et al., 2012) and develop a DC algorithm with L_0 -projection to overcome the difficulty of multiple local minimizers of (14). Specifically, at $(t+1)$ th iteration, we solve a penalized version of (14),

$$\tilde{\mathbf{V}}_{\bullet j}^{t+1} = \arg \min_{\mathbf{V}_{\bullet j}} (2n)^{-1} \sum_{i=1}^n (Y_{ij} - \mathbf{V}_{\bullet j}^\top \mathbf{X}_i)^2 + \gamma_j \tau_j \sum_{l=1}^q \mathbf{I}(|\tilde{V}_{lj}^t| \leq \tau_j) |V_{lj}|; \quad j = 1, \dots, p, \quad (15)$$

where $\gamma_j > 0$ is a tuning parameter and \tilde{V}_{lj}^t is the solution of (15) at the t -th iteration. The constrained solution $\hat{\mathbf{V}}_{\bullet j}^{[t+1]}$ is computed by projecting the penalized solution onto the constrained set $\{\|\mathbf{V}_{\bullet j}\|_0 \leq K_j\}$. The DC algorithm iterates until a termination criterion is met (Tao et al., 2005), rendering a sequence of constrained solutions $(\hat{\mathbf{V}}_{\bullet j}^t)_{t \geq 0}$. A final estimate $\hat{\mathbf{V}}_{\bullet j}$ is the one in the sequence $(\hat{\mathbf{V}}_{\bullet j}^t)_{t \geq 0}$, which minimizes $(2n)^{-1} \sum_{i=1}^n (Y_{ij} - \mathbf{V}_{\bullet j}^\top \mathbf{X}_i)^2$.

Algorithm 2: Constrained minimization via DC programming

- 1 **(Initialization)** Specify the tuning parameters $\gamma_j > 0$, $\tau_j > 0$, and $1 \leq K_j \leq q$. Initialize $\hat{\mathbf{V}}_{\bullet j}^0$ with $\|\hat{\mathbf{V}}_{\bullet j}^0\|_0 \leq K_j$.
 - 2 **(Relaxation)** Compute the penalized solution $\tilde{\mathbf{V}}_{\bullet j}^t$ of (15).
 - 3 **(Projection)** Let $S^{[t]} = \{l : |\tilde{V}_{lj}^t| > |\tilde{V}_{(K_j+1)j}^t|\}$, where $|\tilde{V}_{(K_j+1)j}^t|$ is the $(K_j + 1)$ th largest coefficient in absolute value. Set $\hat{\mathbf{V}}_{\bullet j}^t = \arg \min_{\mathbf{V}_{\bullet j}} (2n)^{-1} \sum_{i=1}^n (Y_{ij} - \mathbf{V}_{\bullet j}^\top \mathbf{X}_i)^2$ subject to $V_{lj} = 0$ for $l \notin S^{[t]}$.
 - 4 **(Termination)** Repeat Steps 2-3 until a termination criterion is met. Then set $\hat{\mathbf{V}}_{\bullet j} = \arg \min_{\mathbf{V}_{\bullet j}} (2n)^{-1} \sum_{i=1}^n (Y_{ij} - \mathbf{V}_{\bullet j}^\top \mathbf{X}_i)^2$ such that $\mathbf{V}_{\bullet j} \in (\hat{\mathbf{V}}_{\bullet j}^t)_{t=1}^T$, where T is the iteration index at termination.
-

We are now ready to introduce a *peeling* strategy to estimate $\mathcal{S} = (\mathcal{A}, \mathcal{I})$ based on \mathbf{V} and Proposition 2. This strategy is a bottom-up process establishes a hierarchy of different layers of primary variables by recursively identifying and peeling-off one leaf layer with their associated intervention variables in the graph. It consists of four steps.

1. **Leaf-instrument pairs:** Identify all leaf-instrument $(X_l \rightarrow Y_j)$ pairs satisfying $V_{lj} = 1$ and $V_{lk} = 0$ for $k \neq j$ via (B) of Proposition 2.
2. **Leaf-noninstrument pairs:** Given leaf variable Y_j 's in Step 2, identify all the non-instruments $(X_m \rightarrow Y_j)$, satisfying $V_{mj} \neq 0$ for $m \neq j$.

3. **Ancestral relations:** Given a leaf variable Y_j , identify any ancestral relation $Y_j \rightsquigarrow Y_k$ by Proposition 2 (C) when $\widehat{\mathbf{V}}_{lk}^{[t-1]} \neq 0$ for each instrument $X_l \rightarrow Y_j$ with Y_k peeled-off in iteration $t' \leq t - 1$.
4. **Peeling-off:** Peel-off all the current leaf-instrument $(X_l \rightarrow Y_j)$ pairs by removing the l row and j th columns from the present \mathbf{V} . Repeat Steps 1-3 for the resulting submatrix of \mathbf{V} until all primary variables are removed.

This *peeling* strategy identifies all the immediate parent-child relations as well as the ancestral relations via a chain of immediate parent-child relations. As a result, it also estimates the testable link set D in Definition 2.

In what is to follow, we implement the *peeling* strategy in Algorithm 3 for an estimate $\widehat{\mathbf{V}}$ of \mathbf{V} with minor adjustments as $\|\widehat{\mathbf{V}}_{l' \bullet}\|_0 = 1$ may not hold due to estimation errors.

Algorithm 3: Peeling

- 1 Initialization: $\widehat{\mathbf{V}}^{[1]} = \widehat{\mathbf{V}}$. Begin iteration $t = 1, \dots$: at iteration t ,
 - 2 **(Leaf-instrument pairs)** Identify all leaf-instrument $(X_l \rightarrow Y_j)$ pairs satisfying $l = \arg \min_{\|\widehat{\mathbf{V}}_{l' \bullet}^{[t]}\|_0 \neq 0} \|\widehat{\mathbf{V}}_{l' \bullet}^{[t]}\|_0$ and $j = \arg \max_{j'} |\widehat{\mathbf{V}}_{lj'}^{[t]}|$.
 - 3 **(Leaf-noninstrument pairs)** Given identified leaf variables Y_j in Step 1, identify all leaf-noninstrument $(X_m \rightarrow Y_j)$ pairs, satisfying $\widehat{\mathbf{V}}_{mj}^{[t]} \neq 0$ for $m \neq \arg \min_{\|\widehat{\mathbf{V}}_{l' \bullet}^{[t]}\|_0 \neq 0} \|\widehat{\mathbf{V}}_{l' \bullet}^{[t]}\|_0$.
 - 4 **(Ancestral relations)** For a leaf variable Y_j , identify any ancestral relation $Y_j \rightsquigarrow Y_k$ when $\widehat{\mathbf{V}}_{lk}^{[t-1]} \neq 0$ for each instrument $X_l \rightarrow Y_j$ with Y_k peeled-off in iteration $t' \leq t - 1$.
 - 5 **(Peeling-off)** Remove all the current leaf-instrument $(X_l \rightarrow Y_j)$ pairs by deleting the l th row and j th columns from the present $\widehat{\mathbf{V}}^{[t]}$ to yield $\widehat{\mathbf{V}}^{[t+1]}$.
 - 6 **(Termination)** Repeat Steps 2-5 until all primary variables are removed.
 - 7 **(Reconstruction of \mathcal{S} and D)** Compute $\widehat{\mathcal{S}} = (\widehat{\mathcal{A}}, \widehat{\mathcal{I}})$ and \widehat{D} , where $\widehat{\mathcal{A}} = \{(l, j) : X_l \rightarrow Y_j, \text{ or } X_l \rightarrow Y_k \Rightarrow Y_j\}$ and $\widehat{\mathcal{A}} = \{(k, j) : Y_k \Rightarrow \dots \Rightarrow Y_j\}$. Then $\widehat{D} = \{(k, j) \in F : \widehat{\mathcal{A}} \cup \{(k, j)\} \text{ has no loops}\}$.
-

A detailed illustration of Algorithm 3 is presented in Example 3 of the Appendix. Note that $\widehat{\mathcal{A}}$ consists of all ancestral relations among Y_1, \dots, Y_p . By definition, $\widehat{\mathcal{A}}$ is a superset of directed relations of \mathbf{U} and $\widehat{\mathcal{I}}$ is a superset of interventional relations of \mathbf{W} . Therefore, Algorithm 3 permits reconstructing the true graph and the associated interventions by estimating (\mathbf{U}, \mathbf{W}) through L_0 -constrained regressions given $\widehat{\mathcal{S}} = (\widehat{\mathcal{A}}, \widehat{\mathcal{I}})$ as in (14),

$$\begin{aligned}
 \min_{(\mathbf{U}_{\widehat{\mathcal{A}}(j), j}, \mathbf{W}_{\widehat{\mathcal{I}}(j), j})} & (2n)^{-1} \sum_{i=1}^n (Y_{ij} - \mathbf{U}_{\widehat{\mathcal{A}}(j), j}^\top \mathbf{Y}_{i, \widehat{\mathcal{A}}(j)} - \mathbf{W}_{\widehat{\mathcal{I}}(j), j}^\top \mathbf{X}_{i, \widehat{\mathcal{I}}(j)})^2 \\
 \text{s.t.} & \sum_{k \in \widehat{\mathcal{A}}(j)} \mathbf{I}(U_{kj} \neq 0) \leq K_j.
 \end{aligned} \tag{16}$$

The final estimate $\widehat{\mathbf{U}}_{\bullet j} = (\widehat{\mathbf{U}}_{\widehat{\text{AN}}(j),j}, \mathbf{0}_{\widehat{\text{AN}}(j)^c})$ and $\widehat{\mathbf{W}}_{\bullet j} = (\widehat{\mathbf{W}}_{\widehat{\text{INT}}(j),j}, \mathbf{0}_{\widehat{\text{INT}}(j)^c})$; $j = 1, \dots, p$. See Table 3 of Section 5.

Concerning diagnostics for Assumptions 1A-1C, Assumption 1A can be empirically examined. Note that the estimate $\widehat{\mathbf{S}}$ by Algorithm 3 satisfies Assumptions 1B and 1C, and hence that a violation of Assumption 1B or 1C for the data generating distribution leads to under-fitting of \mathbf{Y} with $\mathbf{U}^\top \mathbf{Y} + \mathbf{W}^\top \mathbf{X}$. A goodness-of-fit test thus can reveal the departure of these conditions.

3.3 Convergence and consistency of causal discovery

Now we introduce some technical assumptions to derive statistical and computational properties of Algorithm 3. Let $(\mathbb{Y}, \mathbb{X}) \in \mathbb{R}^{n \times (p+q)}$ be the data matrix. Denote by $\boldsymbol{\zeta}$ a generic vector and $\boldsymbol{\zeta}_A \in \mathbb{R}^{|A|}$ be the projection of $\boldsymbol{\zeta}$ onto coordinates in A . Let $K_j^0 = \|\mathbf{V}_{\bullet j}^0\|_0$ and $K_{\max}^0 = \max_{1 \leq j \leq p} K_j^0$.

Assumption 2 (Restricted eigenvalues) For a constant $c_1 > 0$,

$$\Lambda_{\min} = \min_{A: |A| \leq 2K_{\max}^0} \min_{\{\boldsymbol{\zeta}: \|\boldsymbol{\zeta}_{A^c}\|_1 \leq 3\|\boldsymbol{\zeta}_A\|_1\}} \frac{\|\mathbb{X}\boldsymbol{\zeta}\|_2^2}{n\|\boldsymbol{\zeta}\|_2^2} \geq c_1.$$

Assumption 3 (Interventions) For a constant $c_2 > 0$,

$$\max \left(\max_{1 \leq l \leq q} n^{-1} (\mathbb{X}^\top \mathbb{X})_{ll}, \max_{A: |A| \leq 2K_{\max}^0} \max_{1 \leq l \leq K_{\max}^0} n((\mathbb{X}_A^\top \mathbb{X}_A)^{-1})_{ll} \right) \leq c_2^2.$$

Assumption 4 (Nuisance signals)

$$\min_{V_{lj}^0 \neq 0} |V_{lj}^0| \geq 100c_1^{-1}c_2 \max_{1 \leq j \leq p} \sqrt{\Omega_{jj} \log(q)/n}. \quad (17)$$

Assumptions 2-3, as a replacement of Assumption 1A, are satisfied with a probability tending to one for isotropic subgaussian or bounded \mathbf{X} (Rudelson and Zhou, 2012). Assumption 2 is a common condition for proving the convergence rate of Lasso regression (Bickel et al., 2009; Zhang et al., 2014). Assumption 4, as an alternative to Assumption 1B, specifies the minimal signal strength over relevant interventions for causal discovery, leading to the reconstruction of ancestral relations. A signal strength requirement like Assumption 4 is a condition for establishing selection consistency in high dimensional variable selection (Fan et al., 2014; Loh et al., 2017; Zhao et al., 2018). Moreover, Assumption 4 can be further relaxed; see Section 7 for discussions.

Theorem 3 (Finite termination and consistent causal discovery) Under Assumptions 1C, 2, 3, 4, if tuning parameters of Algorithm 2 satisfy:

- (1) $\gamma_j \leq \Lambda_{\min}/6$ in (15); $j = 1, \dots, p$,
- (2) $\sqrt{32c_2^2 \Omega_{jj} \log q/n}/\gamma_j \leq \tau_j \leq 0.4 \min_{V_{lj}^0 \neq 0} |V_{lj}^0|$; $j = 1, \dots, p$,
- (3) $K_j = K_j^0$; $j = 1, \dots, p$,

then Algorithm 2 converges to the global minimizer $\hat{\mathbf{V}}_{\bullet,j}$ of (14) in at most $1 + \lceil \log(K_{\max}^0) / \log 4 \rceil$ iterations almost surely, where $\lceil \cdot \rceil$ is the ceiling function. Moreover, Algorithm 3 recovers the true ancestral relations and relevant interventions $\mathcal{S}^0 = (\mathcal{A}^0, \mathcal{I}^0)$ with $P(\hat{\mathcal{S}} \neq \mathcal{S}^0) \leq 4q^{-2}$, implying that $\hat{\mathcal{S}} = \mathcal{S}^0$ and $\hat{D} = D^0$ almost surely as $n, p, q \rightarrow \infty$.

Algorithm 2 terminates in a finite number of iterations, where the number of iterations depends only on the sparsity K_{\max}^0 . The computational complexity of Algorithm 2 is the number of iterations multiplied by that of solving a weighted Lasso regression, $\log(K_{\max}^0) \times O(q^3 + nq^2)$ (Efron et al., 2004). Importantly, Algorithm 3 correctly identifies $\mathcal{S}^0 = (\mathcal{A}^0, \mathcal{I}^0)$, the set of ancestral relations and that of relevant interventions of each primary variable, in addition to consistent estimation of the set of testable links D^0 for the true graph. Finally, note that Theorem 3 does not apply to observational data ($\mathbf{W} = \mathbf{0}$). In a sense, interventions play an essential role.

4. Inferential theory

This section provides the theoretical justification for the proposed tests.

Assumption 5 (Hypothesis-specific dimension restriction) For a constant $0 < \rho < 1$,

$$\max_{j: \exists (k,j) \in D} \frac{|\text{AN}(j)| + |\text{INT}(j)|}{n} \leq \rho, \quad \text{as } n, p, q \rightarrow \infty.$$

Assumption 5 is a local condition restricting the underlying problem's size. Usually, $|\text{INT}(j)| = O(1)$ and $|\text{AN}(j)| \ll p$; $j = 1, \dots, p$, which dramatically relaxes the condition $n \gg |D|^{1/2}(|D| + p) \log(p)$ for the constrained likelihood ratio test (Li et al., 2019).

Theorem 4 (Empirical p-values) Suppose Assumptions 1C, 2, 3, 4, 5 are met. Moreover, if the tuning parameters in Algorithm 3 satisfy (1)-(3) in Theorem 3 and perturbation size $\delta \in (0, \delta_0]$ with $\delta_0^2 = \min_{1 \leq j \leq p} 0.5\sigma_j^{-2} \left(\frac{(\tau_j^*)^2 c_1^2 n}{90c_2^2(K_j^0 - K_j^* + 1) \log q} - \Omega_{jj} \right) > 0$, whose positivity is ensured by Assumption 4. Then,

(A) (Directed linkage test (2))

$$\begin{aligned} \lim_{\substack{n, p, q \rightarrow \infty \\ \theta^0 \text{ satisfies } H_0 \text{ in (2)}}} \lim_{M \rightarrow \infty} P_{\theta^0}(\text{Pval} < \alpha) &= \alpha, \quad \text{if } H_0 \text{ is testable;} \\ \lim_{\substack{n, p, q \rightarrow \infty \\ \theta^0 \text{ satisfies } H_0 \text{ in (2)}}} \lim_{M \rightarrow \infty} P_{\theta^0}(\text{Pval} = 1) &= 1, \quad \text{if } H_0 \text{ is not testable.} \end{aligned}$$

(B) (Directed pathway test (3))

$$\begin{aligned} \limsup_{\substack{n, p, q \rightarrow \infty \\ \theta^0 \text{ satisfies } H_0 \text{ in (3)}}} \lim_{M \rightarrow \infty} P_{\theta^0}(\text{Pval} < \alpha) &= \alpha, \quad \text{if } H_0 \text{ is testable with } |D| = |F|; \\ \limsup_{\substack{n, p, q \rightarrow \infty \\ \theta^0 \text{ satisfies } H_0 \text{ in (3)}}} \lim_{M \rightarrow \infty} P_{\theta^0}(\text{Pval} = 1) &= 1, \quad \text{if } |D| < |F|. \end{aligned}$$

By Theorem 4, the DP likelihood ratio test yields a valid p-value for (2) and (3). Note that $|D|$ is permitted to depend on n, p, q . Moreover, Proposition 5 summarizes the asymptotics for directed linkage test (2).

Proposition 5 (Asymptotic distribution of Lr of (2)) *Assume that the assumptions of Theorem 4 are met. Under H_0 , as $n, p, q \rightarrow \infty$,*

$$\begin{aligned} 2\text{Lr} &\xrightarrow{d} \chi_{|D|}^2, \text{ if } H_0 \text{ is testable with } |D| > 0 \text{ is fixed;} \\ \frac{2\text{Lr} - |D|}{\sqrt{2|D|}} &\xrightarrow{d} N(0, 1), \text{ if } H_0 \text{ is testable with } |D| \rightarrow \infty, \quad \frac{|D| \log |D|}{n} \rightarrow 0. \end{aligned}$$

Next, we analyze the local limit power of the proposed tests for (2) and (3). Assume $\theta^0 = (\mathbf{U}^0, \mathbf{W}^0, \Sigma^0)$ satisfies H_0 . Let $\mathbf{H} \in \mathbb{R}^{p \times p}$ satisfy $\mathbf{H}_{D^c} = \mathbf{0}$ so that $\mathbf{U}^0 + \mathbf{H}$ is also a DAG adjacency matrix. For testable H_0 , we consider an alternative H_a : $\mathbf{U}_F = \mathbf{U}_F^0 + \mathbf{H}_F$, and define the power function as

$$\beta(\theta^0, \mathbf{H}) = P_{H_a}(\text{Pval} < \alpha). \quad (18)$$

LOCAL POWER OF DIRECTED LINKAGE TEST (2)

Let $\|\mathbf{H}\|_{\text{Fr}} = \|\mathbf{H}_F\|_{\text{Fr}} = n^{-1/2}h$ if $|D| > 0$ is fixed and $\|\mathbf{H}\|_{\text{Fr}} = |D|^{1/4}n^{-1/2}h$ if $|D| \rightarrow \infty$, where $h > 0$ and $\|\cdot\|_{\text{Fr}}$ denotes the Frobenius norm of a matrix.

Proposition 6 (Local power of linkage test (2)) *Assume that H_0 is testable. If the assumptions of Theorem 4 are met, then under H_a , as $n, p, q, M \rightarrow \infty$,*

$$\beta(\theta^0, \mathbf{H}) \geq \begin{cases} P\left(\|\mathbf{Z} + c_l \sqrt{n} \mathbf{H}\|_2^2 > \chi_{|D|, 1-\alpha}^2\right) & \text{if } |D| > 0 \text{ is fixed;} \\ P\left(Z > z_{1-\alpha} - c_l \|\mathbf{H}\|_2^2 / \sqrt{2|D|}\right) & \text{if } |D| \rightarrow \infty, \frac{|D| \log |D|}{n} \rightarrow 0, \end{cases}$$

where $\mathbf{Z} \sim N(\mathbf{0}, \mathbf{I}_{|D|})$ and $Z \sim N(0, 1)$. In particular, $\lim_{h \rightarrow \infty} \beta(\theta^0, \mathbf{H}) = 1$.

LOCAL POWER OF PATHWAY TEST (3)

Let $\min_{(i,j) \in F} |U_{ij}^0 + H_{ij}| = n^{-1/2}h$ if $|F| > 0$ is fixed and $\min_{(i,j) \in F} |U_{ij}^0 + H_{ij}| = n^{-1/2}h \sqrt{\log |F|}$ if $|F| \rightarrow \infty$.

Proposition 7 (Local power of pathway test (3)) *Assume that H_0 is testable. If the assumptions of Theorem 4 are met, then under H_a , as $n, p, q, M \rightarrow \infty$,*

$$\beta(\theta^0, \mathbf{H}) \geq 1 - \frac{|F|}{\sqrt{2\pi}} e^{-(h \sqrt{\log |F|} / \max_{j=1}^p \Omega_{jj} - \sqrt{\chi_{1, 1-\alpha}^2})^2 / 2},$$

where $Z \sim N(h^2 / \max_{j=1}^p \Omega_{jj}, 1)$. Then, $\lim_{h \rightarrow \infty} \beta(\theta^0, \mathbf{H}) = 1$.

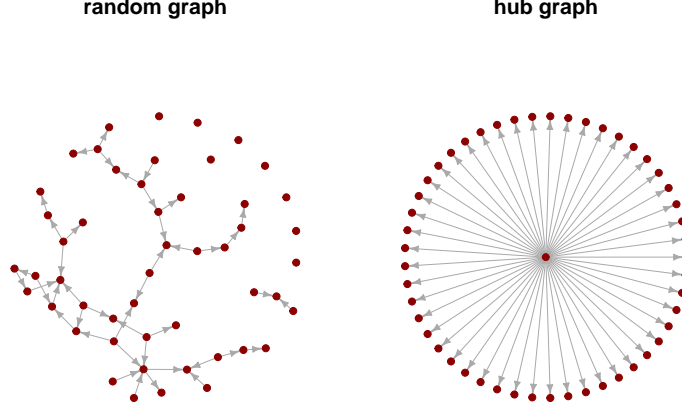


Figure 2: Two types of graphs used in Simulations 1-2.

5. Simulations

This section examines the operating characteristics of the DP modified likelihood ratio test (DP-MLR) as described in Algorithm 1 and compares the test with the standard likelihood ratio based on estimated $\hat{\mathcal{S}}$ (LR), the modified oracle likelihood ratio test (M-OLR), and the oracle likelihood ratio test (OLR) regarding empirical sizes and powers in simulated examples. Here LR uses $\text{Lr}(\hat{\mathcal{S}}, \hat{\Sigma}_{\text{unadj}})$ in (6) without the adjusted degrees of freedom in (7), while OLR uses $\text{Lr}(\mathcal{S}^0, \hat{\Sigma}_{\text{unadj}})$ assuming that the true $\mathcal{S}^0 = (\mathcal{A}^0, \mathcal{I}^0)$ were known in advance and M-OLR uses $\text{Lr}(\mathcal{S}^0, \hat{\Sigma})$ and (7) to adjust the degrees of freedom. The p-values of LR, M-OLR and OLR are $1 - \hat{F}_{\text{Lr}}(\text{Lr})$ for (2) and $\max_{\nu} (1 - \hat{F}_{\text{Lr}\nu}(\text{Lr}_{\nu}))$ for (3), where the null distribution of \hat{F}_{Lr} and $\hat{F}_{\text{Lr}\nu}$ is computed using an asymptotic approximation of either the χ^2 or the normal distribution in Proposition 5 with an estimate \hat{D} obtained by Algorithm 3.

For the proposed DP-MLR, we fix the Monte Carlo sample size $M = 1000$ and $\delta = 1$ in Algorithm 1. Our limited experience suggests that results are insensitive to the choice of $\delta = 1$ and $M = 1000$ suffices. In Algorithm 2, we fix $\tau_j = 0.2$ and tune parameters $\gamma_j = \gamma \in \{0.05, \dots, 2\}$ (50 values, equally spaced) and $K_j \in \{1, \dots, 30\}$; $j = 1, \dots, p$ by minimizing the five-fold prediction criterion $\sum_{i \in \mathcal{Z}^l} (Y_{ij} - (\hat{\mathbf{V}}_{\bullet j}^{-l})^\top \mathbf{X}_i)^2$, where $\hat{\mathbf{V}}_{\bullet j}^{-l}$ are the estimates based on $\mathcal{Z} \setminus \mathcal{Z}^l$, and $(\mathcal{Z}^l)_{l=1}^5$ is a random partition of the original data \mathcal{Z} with roughly equal parts. Then the optimal tuning parameters K_j ; $j = 1, \dots, p$, are used to perform a test based on \mathcal{Z} .

We produce numerical results in our developed R package `intdag`, interfacing with C++ code for implementing the proposed tests based on Algorithms 1-3.

TEST OF DIRECTED LINKAGES

For (2), with $(k_0, j_0) = (2, p)$, we examine two different hypotheses: (i) $H_0 : U_{k_0 j_0} = 0$ versus $H_a : U_{k_0 j_0} \neq 0$; (ii) $H_0 : U_F = 0$ versus $H_a : U_F \neq 0$; $F = \{(k, p) : k = 2, \dots, 51\}$. Whereas the first concerns one single entry of \mathbf{U} , the second focuses on the last column of

U . Moreover, three alternatives $H_a : U_{k_0 j_0} = 0.1l$ and $U_{kj} = 0$ for $(k, j) \in F \setminus \{(k_0, j_0)\}$; $l = 1, 2, 3$ are used for the power analysis in (i) and (ii).

TEST OF DIRECTED PATHWAYS

For (3), we examine the hypothesis: $H_0 : U_{kj} = 0$ for some $(k, j) \in F$ versus $H_a : U_{kj} \neq 0$ for all $(k, j) \in F = \{(1, j) : j = 2, \dots, 11\}$. Specifically, the data are generated under a graph satisfying H_0 , where $U_{12} = 0$ and $U_{1,j} = 1$; $j = 3, \dots, 11$. Three alternatives $H_a : U_{kj} = 0.1l$ for all $(k, j) \in F$; $l = 1, 2, 3$ are used for the power analysis.

In simulations, two types of graphs are considered, including random and hub DAGs, as displayed in Figure 2. For the empirical size of a test, we compute the percentage of times rejecting H_0 out of 1000 simulations when H_0 is true. For the empirical power of a test, we report the percentage of times rejecting H_0 out of 100 simulations when H_a is true under three alternative hypotheses H_a .

Table 1: Empirical sizes and powers of modified and oracle likelihood ratio tests for testing linkages (2) with the sample size $n = 300$. Here DP-MLR and LR denote the proposed modified and standard likelihood ratio tests, while M-OLR and OLR refer to as the corresponding modified and standard oracle tests provided that the graph structure were known in advance, where LR uses the chi-square or normal approximations for the null distribution with estimated $|\hat{D}|$ and $\alpha = 0.05$ is used.

$\mathcal{G}, D $	(p, q, n)	DP-MLR	LR	M-OLR	OLR
		size (power)	size (power)	size (power)	size (power)
Ran, 1	(75, 100, 300)	.045 (.61, 1.0, 1.0)	.051 (.61, 1.0, 1.0)	.047 (.59, .99, 1.0)	.048 (.66, 1.0, 1.0)
	(150, 200, 300)	.047 (.53, 1.0, 1.0)	.049 (.54, 1.0, 1.0)	.044 (.50, 1.0, 1.0)	.056 (.59, 1.0, 1.0)
	(300, 300, 300)	.055 (.55, .98, 1.0)	.058 (.56, .98, 1.0)	.050 (.55, .99, 1.0)	.061 (.55, 1.0, 1.0)
Ran, 50	(75, 100, 300)	.046 (.13, .46, .88)	.087 (.22, .58, .96)	.052 (.13, .48, .88)	.093 (.24, .63, 1.0)
	(150, 200, 300)	.049 (.09, .44, .83)	.077 (.23, .60, .94)	.057 (.12, .43, .85)	.090 (.23, .59, 1.0)
	(300, 300, 300)	.053 (.13, .50, .84)	.114 (.26, .69, .91)	.055 (.15, .56, .84)	.102 (.21, .64, 1.0)
Hub, 1	(75, 100, 300)	.050 (.59, .99, 1.0)	.052 (.61, .99, 1.0)	.049 (.57, 1.0, 1.0)	.053 (.64, 1.0, 1.0)
	(150, 200, 300)	.051 (.52, .98, 1.0)	.054 (.53, .98, 1.0)	.051 (.57, 1.0, 1.0)	.055 (.52, 1.0, 1.0)
	(300, 300, 300)	.047 (.54, .99, 1.0)	.055 (.57, 1.0, 1.0)	.046 (.60, 1.0, 1.0)	.052 (.57, 1.0, 1.0)
Hub, 50	(75, 100, 300)	.051 (.10, .33, .86)	.080 (.17, .56, .95)	.054 (.09, .42, .90)	.084 (.20, .51, .96)
	(150, 200, 300)	.058 (.15, .42, .83)	.096 (.24, .64, .93)	.055 (.15, .39, .83)	.091 (.23, .58, .95)
	(300, 300, 300)	.054 (.12, .47, .88)	.092 (.22, .69, .98)	.048 (.14, .52, .92)	.086 (.26, .65, .98)

Simulation 1 (Random graph) This example generates a random DAG of p primary variables and q intervention variables. For U , upper off-diagonal entries of U are sampled randomly from $\{0, 1\}$ according to the Bernoulli distribution with a success probability $1/p$ and the other entries of U are zero. We modify U according to H_0 and H_a . This upper triangular matrix U represents a DAG. Then the intervention coefficient matrix W is set as follows: $W_{jj} = 1$; $j = 1, \dots, p$ and $W_{lj} = 0$; $1 \leq l \neq j \leq q$. For $\Sigma = \text{Diag}(\sigma_1^2, \dots, \sigma_p^2)$, we set $\sigma_1^2, \dots, \sigma_p^2$ to be equally spaced from 0.5 to 1. For interventions, we generate binary intervention variables $\mathbf{X} = (X_1, \dots, X_q)^\top$ by first sampling a latent variable $Z \sim N(0, 1)$ and then sampling $X_l \in \{1, -1\}$ independently with $P(X_l = 1) = e^Z / (1 + e^Z)$ and $P(X_l = -1) = 1 / (1 + e^Z)$; $l = 1, \dots, q$. Fixing (U, W, Σ) , we generate 1000 random samples according to (1) under H_0 and 100 random samples under H_a .

Table 2: Empirical sizes and powers of modified and oracle likelihood ratio tests for testing pathways (3) with the sample size $n = 300$. Here DP-MLR and LR denote the proposed modified and standard likelihood ratio tests, while M-OLR and OLR refer to as the corresponding modified and standard oracle tests provided that the graph structure were known in advance, where LR uses the chi-square or normal approximations for the null distribution with estimated $|\hat{D}|$ and $\alpha = 0.05$ is used.

$\mathcal{G}, D $	(p, q, n)	DP-MLR	LR	M-OLR	OLR
		size (power)	size (power)	size (power)	size (power)
Ran, 10	(75, 100, 300)	.048 (.12, .99, 1.0)	.050 (.12, 1.0, 1.0)	.046 (.15, 1.0, 1.0)	.051 (.17, 1.0, 1.0)
	(150, 200, 300)	.045 (.09, 1.0, 1.0)	.049 (.13, 1.0, 1.0)	.050 (.13, 1.0, 1.0)	.049 (.14, 1.0, 1.0)
	(300, 300, 300)	.051 (.16, 1.0, 1.0)	.054 (.18, 1.0, 1.0)	.051 (.20, 1.0, 1.0)	.056 (.20, 1.0, 1.0)
Hub, 10	(75, 100, 300)	.049 (.16, .99, 1.0)	.052 (.18, .99, 1.0)	.055 (.15, .99, 1.0)	.052 (.18, 1.0, 1.0)
	(150, 200, 300)	.050 (.18, .99, 1.0)	.051 (.18, .99, 1.0)	.054 (.19, 1.0, 1.0)	.055 (.22, 1.0, 1.0)
	(300, 300, 300)	.042 (.14, 1.0, 1.0)	.046 (.15, 1.0, 1.0)	.040 (.12, 1.0, 1.0)	.047 (.16, 1.0, 1.0)

Table 3: Structural Hamming distance (SHD) as well as its standard deviation (in parenthesis) of causal discovery results based on Algorithm 3 for random and hub graphs in Simulations 1-2 over 1000 runs. A small value of SHD indicates a better result, where $\text{SHD}(\hat{\mathbf{U}}, \mathbf{U}^0) = \sum_{k,j} |\mathbf{I}(\hat{U}_{kj} \neq 0) - \mathbf{I}(U_{kj}^0 \neq 0)|$ and $\text{SHD}(\hat{\mathbf{W}}, \mathbf{W}^0) = \sum_{l,j} |\mathbf{I}(\hat{W}_{lj} \neq 0) - \mathbf{I}(W_{lj}^0 \neq 0)|$ measure the distances between estimated and true adjacency matrices $\hat{\mathbf{U}}$ and \mathbf{U}^0 and estimated and true intervention matrices $\hat{\mathbf{W}}$ and \mathbf{W}^0 , respectively.

\mathcal{G}	(p, q, n)	$\text{SHD}(\hat{\mathbf{U}}, \mathbf{U}^0)$	$\text{SHD}(\hat{\mathbf{W}}, \mathbf{W}^0)$
Ran	(75, 100, 300)	8.7 (4.6)	10.2 (7.9)
	(150, 200, 300)	12.4 (7.2)	15.8 (10.6)
	(300, 300, 300)	13.4 (9.1)	20.3 (12.5)
Hub	(75, 100, 300)	.6 (.6)	1.5 (.9)
	(150, 200, 300)	.8 (1.0)	1.9 (1.3)
	(300, 300, 300)	1.2 (.9)	2.6 (1.6)

Simulation 2 (Hub graph) *This example generates a hub DAG of p primary variables and q intervention variables in the same setup of Simulation 1 except for \mathbf{U} . Specifically, an adjacency matrix \mathbf{U} is set to be $U_{1j} = 1; j = 2, \dots, p$, and $U_{kj} = 0$ otherwise, $1 \leq k, j \leq p$. This generates a sparse graph with a dense neighborhood of the first node.*

As suggested by Tables 1 and 2, the proposed DP modified likelihood test, DP-MLR, performs well for testing directed linkages (2) and pathways (3) in Simulations 1-2. Its empirical sizes are close to the nominal level $\alpha = 0.05$ in all scenarios, while its powers increase to 1 as a test's level of difficulty decreases under H_a . The DP test, DP-MLR, nearly matches the result of the modified oracle likelihood ratio test M-OLR using the true graph structure. The standard likelihood ratio test, LR, appears overly optimistic with an inflated Type I error. Moreover, an adjustment of the degrees of freedom makes a difference for testing (2) when $|D| = 50$, comparing M-OLR and OLR. DP-MLR is comparable with the corresponding oracle test, M-OLR, suggesting that the DP scheme performs well for approximating the null distribution of the modified likelihood ratio.

Concerning causal discovery and identification of relevant interventions, the proposed peeling method performs well for both the random and hub graphs, as measured by the structural Hamming distance in Table 3.

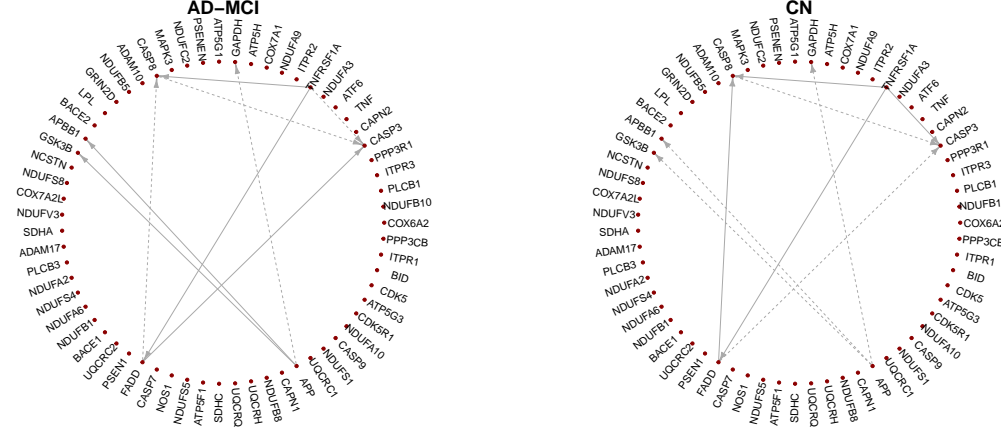


Figure 3: Display of all genes and the subnetworks associated with genes APP and CASP3 tested by the proposed test (2). Solid/dashed arrows indicate significant/insignificant linkages at $\alpha = 0.05$ after adjustment for multiplicity by the Bonferroni-Holm correction.

Overall, the simulation result is consistent with the theoretical results.

6. ADNI data analysis

This section applies the proposed tests to analyze an Alzheimer’s Disease Neuroimaging Initiative (ADNI) dataset. In particular, we infer gene pathways related to Alzheimer’s Disease (AD) to highlight some gene-gene interactions differentiating patients with AD/cognitive impairments and healthy individuals.

The raw data are available in the ADNI database (adni.loni.usc.edu), including gene expression, whole-genome sequencing, and phenotypic data. After cleaning and merging, we have a sample size of 712 subjects. From the KEGG database (Kanehisa and Goto, 2000), we extract the AD reference pathway (hsa05010), including 146 genes in the ADNI data.

For data analysis, we first regress the gene expression levels on five covariates—gender, handedness, education level, age, and intracranial volume, then use the residuals as gene expressions in the following analysis. Next, we extract genes and their most correlated two SNPs such that each gene has at least one significant SNP at a significance level below 10^{-3} . This extraction yields $p = 63$ genes as primary variables and $q = 2p = 126$ SNPs as intervention variables, which we treat as unspecified interventions in our data analysis. Then all gene expression levels are normalized.

The dataset contains individuals in four groups, namely, Alzheimer’s Disease (AD), Early Mild Cognitive Impairment (EMCI), Late Mild Cognitive Impairment (LMCI), and Cognitive Normal (CN). For our purpose, we treat 247 CN individuals as controls while the remaining 465 individuals as cases (AD-MCI). Then, we use the gene expressions and the SNPs to infer gene pathways for 465 AD-MCI and 247 CN control cases, respectively.

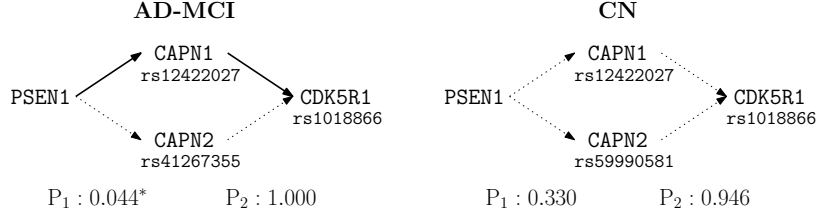


Figure 4: P-values of pathway tests (3) as well as identified SNPs by the proposed tests for the AD-MCI and CN groups, where p-values are adjusted for multiplicity by the Bonferroni-Holm correction and solid/dashed arrows indicate significant/insignificant pathways at $\alpha = 0.05$, labeled by the location of a SNP.

In the literature, genes APP, CASP3, and PSEN1 are well-known to be associated with AD (Goate et al., 1991; Gervais et al., 1999). For this dataset, we thus focus attention on the regulatory subnetwork associated with genes APP, CASP3, and PSEN1 in the KEGG AD reference pathway (hsa05010). First, we consider a hypothesis test of linkages $H_0 : U_{kj} = 0$ for all $(k, j) \in F$ versus $H_a : U_{kj} \neq 0$ for some $(k, j) \in F$, where F consists of nine links as shown in Figure 3. Moreover, we consider two hypothesis tests of pathways $H_0 : U_{kj} = 0$ for some $(k, j) \in P_\ell$ versus $H_a : U_{kj} \neq 0$ for all $(k, j) \in P_\ell$; $\ell = 1, 2$, where the two pathways are specified by $P_1 = \{\text{PSEN1} \rightarrow \text{CAPN1} \rightarrow \text{CDK5R1}\}$, and $P_2 = \{\text{PSEN1} \rightarrow \text{CAPN2} \rightarrow \text{CDK5R1}\}$. See Figure 4.

In Figures 3-4, the p-values and significant results under the significance level $\alpha = 0.05$ after the Holm-Bonferroni adjustment for $2 \times (9 + 2) = 22$ tests are displayed. In Figures 3, the linkage test (2) exhibits a strong evidence for the presence of connections $\{\text{APP} \rightarrow \text{APBB1}, \text{APP} \rightarrow \text{GSK3B}, \text{FADD} \rightarrow \text{CASP3}\}$ in the AD-MCI group, but no evidence of their presence in the CN group. Meanwhile, the linkage test suggests the presence of connections $\{\text{TNFRSF1A} \rightarrow \text{CASP3}, \text{FADD} \rightarrow \text{CASP8}\}$ in the CN group, but not so in the AD-MCI group. In both groups, we identify the linkages $\{\text{TNFRSF1A} \rightarrow \text{FADD}, \text{TNFRSF1A} \rightarrow \text{CASP8}\}$. Moreover, in Figure 4, the pathway test (3) supports the presence of a pathway $\{\text{PSEN1} \rightarrow \text{CAPN1} \rightarrow \text{CDK5R1}\}$ in the AD-MCI group (p-value = 0.042) but not in the CN group (with a p-value of 0.36). The pathway $\{\text{PSEN1} \rightarrow \text{CAPN2} \rightarrow \text{CDK5R1}\}$ appears insignificant at $\alpha = 0.05$ for both groups. Also noted is that one of our discoveries is consistent with the literature: according to the AlzGene database (alzgene.org), GSK3B differentiates AD patients from normal subjects; as shown in Figures 3-4, our analysis indicates the presence of connection $\text{APP} \rightarrow \text{GSK3B}$ for the AD-MCI group, but not for the CN group, the former of which is confirmed by Figure 1 of (Vanleuven, 2011). We confirm that the SNPs have strong intervention effects on the AD-MCI and CN groups, with the median p-value of 8.6×10^{-4} and 4.7×10^{-4} . Finally, as suggested by Figure 5, the normality assumption in (1) is adequate for both groups.

In summary, our analysis suggests that the regulatory network of genes APP, CASP3, and PSEN1 appears to differ between the AD-MCI and CN groups. In particular, the subnetwork associated with APP and CASP3 in Figure 3 and the pathway $\{\text{PSEN1} \rightarrow \text{CAPN1} \rightarrow \text{CDK5R1}\}$ in Figure 4 seem to differentiate the two groups. More studies are required to confirm this discovery.

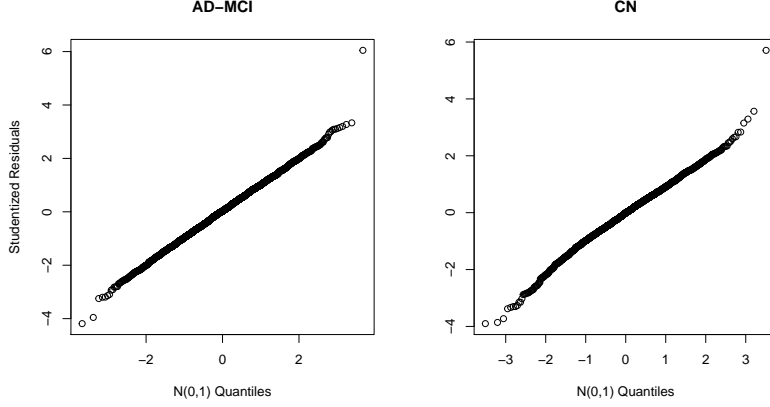


Figure 5: Normal quantile-quantile plots of studentized residuals of the AD-MCI and CN groups.

7. Discussions

This article proposes estimation and inference methods for a directed Gaussian graphical model with interventions, where the targets and strengths of interventions are unknown.

7.1 Simultaneous testing for multiple directed relations

First, the modified DP likelihood ratio test is derived based on estimated ancestral relations and instrumental and non-instrumental interventions. This test accounts for the statistical uncertainty of identification based on a novel data perturbation scheme. The inference requires the knowledge of ancestral relations defined by the null hypothesis as well as relevant interventions. Second, we develop a peeling algorithm for consistent causal discovery, particularly identifying the ancestral relations and relevant interventions. Third, we derive a theory justifying the proposed tests and the data perturbation scheme. To our knowledge, this is the first attempt at a formal hypothesis testing of the directionality and strength of directed relations jointly in a high-dimensional situation. Moreover, we prove that the DC algorithm is a low-order polynomial algorithm that finds a global minimizer almost surely under the data generating distribution. Finally, we apply the proposed tests to gene network analysis to demonstrate its utility.

7.2 Selection consistency

Assumption 4 in Theorem 3 leads to consistent identification for \mathbf{V} . However, it is unnecessary for consistent reconstruction of ancestral relations as illustrated in Example 3 in the Appendix. In fact, it can be further relaxed by a less intuitive condition, Assumption 6, which requires the consistent identification only for *relevant interventions* ($X_l \Rightarrow Y_j$).

Assumption 6 *There exists K_j^* with $|\text{INT}(j)| \leq K_j^* \leq K_j^0$ such that*

$$\min_{l: X_l \Rightarrow Y_j} |V_{lj}^0| \geq \tau_j^* \equiv |\mathbf{V}_{\bullet j}^0|_{(K_j^*)} \geq 100c_1^{-1}c_2\sqrt{\Omega_{jj}(K_j^0 - K_j^* + 1)\log q/n}, \quad (19)$$

where $|\mathbf{V}_{\bullet j}^0|_{(K_j^*)}$ denotes the K_j^* th largest coefficient of $\mathbf{V}_{\bullet j}^0$ in the absolute value; $j = 1, \dots, p$.

Theorem 8 Under Assumptions 1C, 2, 3, 6, if tuning parameters of Algorithm 2 satisfy:

- (1) $\gamma_j \leq \Lambda_{\min}/6\sqrt{K_j^0 - K_j^* + 1}$ in (15); $j = 1, \dots, p$,
- (2) $\sqrt{32c_2^2\Omega_{jj}\log q/n}/\gamma_j \leq \tau_j \leq 0.4\tau_j^*$; $j = 1, \dots, p$,
- (3) $K_j = K_j^*$; $j = 1, \dots, p$,

then Algorithm 2 terminates in at most $1 + \lceil \log(K_{\max}^0)/\log 4 \rceil$ iterations, where $\lceil \cdot \rceil$ is the ceiling function. Moreover, $\hat{\mathcal{S}} = \mathcal{S}^0$ and $\hat{D} = D^0$ almost surely as $n, p, q \rightarrow \infty$.

7.3 Faithfulness

In the literature, a faithfulness condition is usually assumed for identifiability up to Markov equivalence classes (Spirtes et al., 2000), as defined in (25) with $\kappa = 0$ in the Appendix in the context of the Gaussian graphical model. Such an assumption appears not comparable to Assumption 1 required for the identifiability of model (1). Concerning causal discovery, faithfulness is inadequate for consistent estimation, particularly in a high-dimensional situation. Strong faithfulness, as defined in (25) in the Appendix, is often assumed for the algorithms based on faithfulness; see Uhler et al. (2013). As shown in Uhler et al. (2013), strong faithfulness can be very restrictive, especially for a large Gaussian directed acyclic graph. By comparison, Algorithm 3 yields causal discovery based on Assumption 4 instead of strong faithfulness. In some sense, Assumption 4 (or 6) requires the sufficient signal strength that is analogous to the condition for consistent feature selection (Shen et al., 2012). This assumption may be thought of as an alternative to strong faithfulness. As illustrated in Example 4 of the Appendix, Assumption 4 (or 6) is less stringent than strong faithfulness. In short, Algorithm 3 bridges the gap between model identifiability and causal discovery.

Acknowledgments

We would like to acknowledge support for this project by NSF grants DMS-1712564, DMS-1952539 and NIH grants R01GM113250, R01GM126002, R01HL116720, R01HL105397, R01AG069895, and R01AG065636.

Appendix A. Illustrative examples

Identifiability of model (1) and Assumption 1

The parameter space for model (1) is

$$\{(\mathbf{U}, \mathbf{W}, \mathbf{\Sigma}) : \mathbf{U} \in \mathbb{R}^{p \times p} \text{ represents a DAG, } \mathbf{W} \in \mathbb{R}^{p \times q}, \mathbf{\Sigma} = \text{diag}(\sigma_1^2, \dots, \sigma_p^2)\}.$$

As suggested by Proposition 1, Assumption 1 (1A-1C) suffices for identification of every parameter value in the parameter space. Next, we show by examples that if Assumption 1B or 1C is violated then model (1) is no longer identifiable.

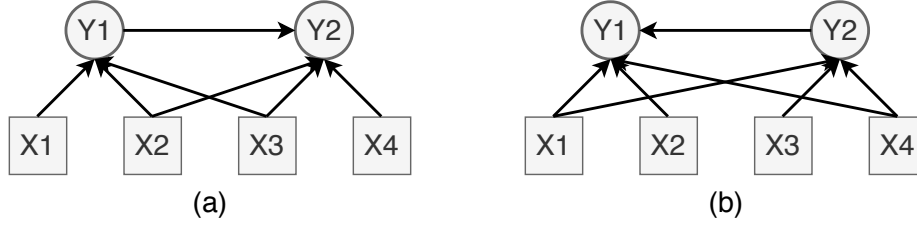


Figure 6: (a) Display of DAG graph defined by (20). (b) Display of DAG graph defined by (21).

Example 2 (Identifiability) In model (1), consider two non-identifiable bivariate situations: (1) $p = 2$ and $q = 4$ and (2) $p = 2$ and $q = 2$.

- (1) Model (1) is nonidentifiable when Assumption 1B breaks down. Consider two different models with different parameter values:

$$\boldsymbol{\theta} : \quad Y_1 = X_1 + X_2 + X_3 + \varepsilon_1, \quad Y_2 = Y_1 - X_2 + X_3 + X_4 + \varepsilon_2 \quad (20)$$

$$\tilde{\boldsymbol{\theta}} : \quad Y_1 = 0.5Y_2 + 0.5X_1 + X_2 - 0.5X_4 + \tilde{\varepsilon}_1, \quad Y_2 = X_1 + 2X_3 + X_4 + \tilde{\varepsilon}_2, \quad (21)$$

where ε_1 and ε_2 are independent and identically distributed $N(0, 1)$, $\tilde{\varepsilon}_1 \sim N(0, 0.5)$ and $\tilde{\varepsilon}_2 \sim N(0, 2)$ are independent. As depicted in Figure 6, (20) satisfies Assumption 1C. However, Assumption 1B is violated given that $\text{Cov}(Y_2, X_2 \mid \mathbf{X}_{\{1,3,4\}}) = 0$ and X_2 is non-instrumental. This is because the direct interventional effect of X_2 on Y_2 cancels out its indirect interventional effect through Y_2 's immediate parent Y_1 . Similarly, (21) satisfies Assumption 1C but $\text{Cov}(Y_1, X_4 \mid \mathbf{X}_{\{1,2,3\}}) = 0$ violating Assumption 1B. In this case, it can be verified that $\boldsymbol{\theta}$ and $\tilde{\boldsymbol{\theta}}$ correspond to the same distribution of \mathbf{Y} given \mathbf{X} because they share the same $(\mathbf{V}, \boldsymbol{\Omega})$ in (13) even with different values of $(\mathbf{U}, \mathbf{W}, \boldsymbol{\Sigma})$. Hence, it is impossible to infer the directed relation between Y_1 and Y_2 .

- (2) Model (1) is nonidentifiable when Assumption 1C breaks down. Consider two different models with different parameter values:

$$\boldsymbol{\theta} : \quad Y_1 = X_1 + X_2 + \varepsilon_1, \quad Y_2 = Y_1 + X_2 + \varepsilon_2, \quad (22)$$

$$\tilde{\boldsymbol{\theta}} : \quad Y_1 = 0.5Y_2 + 0.5X_1 + \tilde{\varepsilon}_1, \quad Y_2 = X_1 + 2X_2 + \tilde{\varepsilon}_2, \quad (23)$$

where ε_1 and ε_2 are independent and identically distributed $N(0, 1)$, and $\tilde{\varepsilon}_1 \sim N(0, 0.5)$ and $\tilde{\varepsilon}_2 \sim N(0, 2)$ are independent. As described in Figure 7, (22) and (23) satisfy Assumption 1B. In (22), Y_2 does not have any instrumental intervention although it has a non-instrumental intervention X_2 . Similarly, in (23), neither does Y_1 have any instrumental intervention while having a non-instrumental intervention X_2 . As in the previous case, $\boldsymbol{\theta}$ and $\tilde{\boldsymbol{\theta}}$ yield the same distribution of \mathbf{Y} given \mathbf{X} because they share the same $(\mathbf{V}, \boldsymbol{\Omega})$ in (13) even with different values of $(\mathbf{U}, \mathbf{W}, \boldsymbol{\Sigma})$. In this case, it is impossible to infer the directed relation between Y_1 and Y_2 , given that $\boldsymbol{\theta}$ and $\tilde{\boldsymbol{\theta}}$ encode the same distribution of (\mathbf{Y}, \mathbf{X}) .



Figure 7: (a) Display of DAG graph defined by (22). (b) Display of DAG graph defined by (23).

Illustration of Algorithm 3

We now illustrate Algorithm 3 by Example 3. Note that Algorithm 3 does not require selection consistency of matrix \mathbf{V}^0 .

Example 3 Consider model (1) with $p = q = 5$,

$$\begin{aligned} Y_1 &= X_1 + \varepsilon_1, & Y_2 &= 0.5Y_1 + X_3 + \varepsilon_2, \\ Y_3 &= 0.5Y_2 + X_5 + \varepsilon_3, & Y_4 &= 0.5Y_3 - 0.1Y_1 + X_2 + \varepsilon_4, \\ Y_5 &= X_4 + \varepsilon_5, \end{aligned} \quad (24)$$

where $\varepsilon_1, \dots, \varepsilon_5$ are independent and identically distributed $N(0, 1)$. Then (24) defines a DAG as displayed in Figure 1(a). For illustration, we generate a random sample of size $n = 40$. Compute $\hat{\mathbf{V}}$ by Algorithm 2. In particular,

$$\mathbf{V}^0 = \begin{pmatrix} 1 & 0.5 & 0.25 & 0.025 & 0 \\ 0 & 0 & 0 & 1 & 0 \\ 0 & 1 & 0.5 & 0.25 & 0 \\ 0 & 0 & 0 & 0 & 1 \\ 0 & 0 & 1 & 0.5 & 0 \end{pmatrix}, \quad \hat{\mathbf{V}} = \begin{pmatrix} 0.92 & 0.48 & 0.27 & 0 & 0 \\ 0 & 0 & 0 & 1.08 & 0 \\ 0 & 1.03 & 0.52 & 0.21 & 0 \\ 0 & 0 & 0 & 0 & 1.06 \\ 0 & 0 & 0.98 & 0.55 & 0 \end{pmatrix}.$$

Algorithm 3 proceeds as follows.

- **Iteration 1:** We have the index set of leaf-instruments $\{X_2, X_4\}$. Identification of leaf nodes:

X_2 is identified as an instrument of leaf node Y_4 ($X_2 \rightarrow Y_4$) as $\hat{V}_{24} \neq 0$ is the only nonzero in the row 2 with the smallest row L_0 -norm.

X_4 is identified as an instrument of leaf node Y_5 ($X_4 \rightarrow Y_5$) as $\hat{V}_{45} \neq 0$ is the only nonzero in row 4 with the smallest row L_0 -norm.

Then Y_4 , Y_5 , X_2 , and X_4 are removed.

- **Iteration 2:** We have the index set of leaf-instrument $\{X_5\}$. Identification of leaf nodes:

X_5 is identified as an instrument of a leaf node Y_3 ($X_5 \rightarrow Y_3$) in the subgraph for Y_1, Y_2, Y_3 given that $\hat{V}_{53} \neq 0$ is the only nonzero element in the row with the smallest

row L_0 -norm of the submatrix for Y_1, Y_2, Y_3 . Since $\widehat{V}_{54} \neq 0$ and Y_4 is removed in the last iteration, $Y_3 \Rightarrow Y_4$.

Then Y_3 and X_5 are removed.

- **Iteration 3:** We have the index set of leaf-instrument $\{X_3\}$. Identification of leaf nodes:

X_3 is identified as an instrument of a leaf node Y_2 ($X_3 \rightarrow Y_2$) similarly in the subgraph for Y_1, Y_2 given that $\widehat{V}_{32} \neq 0$ is the largest nonzero element in its row of the submatrix. Since $\widehat{V}_{33} \neq 0$ and Y_3 is removed in the last iteration, $Y_2 \Rightarrow Y_3$.

After, Y_2 and X_3 are removed.

- **Iteration 4:** We have the index set of leaf-instrument $\{X_1\}$. Identification of leaf nodes:

X_1 is an instrument of Y_1 similarly ($X_1 \rightarrow Y_1$). Since $\widehat{V}_{12} \neq 0$ and Y_2 is removed in last iteration, $Y_1 \Rightarrow Y_2$. Then Y_1 and X_1 are removed and the peeling process is terminated.

Finally, Step 7 of Algorithm 3 adds three ancestral relations $Y_1 \rightsquigarrow Y_4$, $Y_1 \rightsquigarrow Y_3$, and $Y_2 \rightsquigarrow Y_4$, in addition to three relevant intervention relations $X_5 \Rightarrow Y_4$, $X_3 \Rightarrow Y_3$, and $X_1 \Rightarrow Y_2$.

Comparison of faithfulness and Assumption 4

According to Uhler et al. (2013), a multivariate Gaussian distribution of $(Z_1, \dots, Z_{p+q})^\top$ is said to be κ -strong faithful to a DAG if

$$\min_{1 \leq i \neq j \leq p+q} \min_{S \subseteq V \setminus \{i, j\}} \{|\text{Corr}(Z_i, Z_j \mid \mathbf{Z}_S)| : Z_i \text{ is not d-separated from } Z_j \mid \mathbf{Z}_S\} > \kappa, \quad (25)$$

where $\kappa \in [0, 1)$, Corr denotes the correlation, and Z_i is d-separated from $Z_j \mid \mathbf{Z}_S$ if \mathbf{Z}_S block every path between Z_i and Z_j ; $i \neq j$ (Pearl, 2000). When $\kappa = 0$, (25) is equivalent to faithfulness. For consistent discovery (up to Markov equivalence classes), it often requires that $\kappa \geq O(\sqrt{s_0 \log(p+q)/n})$, where s_0 is a sparsity measure; see Uhler et al. (2013) for a survey. For a pair (i, j) , the number of possible sets for S is $2^{(p+q-2)}$. If $Z_i \rightarrow Z_j$, then $\text{Corr}(Z_i, Z_j \mid \mathbf{Z}_S) \neq 0$ for any S . Therefore, for this (i, j) pair alone, (25) could require exponentially many conditions. Indeed, (25) is very restrictive (Uhler et al., 2013).

We now briefly discuss the relevance of the strong-faithfulness (25) and Assumption 4 by Example 4.

Example 4 (Faithfulness) For simplicity, assume \mathbf{X} in (1) is normally distributed $N(\mathbf{0}, \mathbf{I})$. Consider model (1) with $p = q = 3$,

$$Y_1 = W_{11}X_1 + \varepsilon_1, \quad Y_2 = U_{12}Y_1 + W_{22}X_2 + \varepsilon_2, \quad Y_3 = U_{13}Y_1 + U_{23}Y_2 + W_{33}X_3 + \varepsilon_3,$$

where $\varepsilon_1, \varepsilon_2, \varepsilon_3 \sim N(0, 1)$ are independent and $U_{12}, U_{13}, U_{23}, W_{11}, W_{22}, W_{33} \neq 0$. Note that causal relations among \mathbf{X} are not of interest. Let $\mathbf{Z} = (Y_1, Y_2, Y_3, X_1, X_2, X_3)^\top$. Then (25)

becomes

$$\begin{aligned} & \min_{S_1 \subseteq \{i,j\}^c, S_2} \{|\text{Corr}(Y_i, Y_j \mid \mathbf{Z}_S)| : Y_i \text{ is not } d\text{-separated from } Y_j \mid \mathbf{Z}_S = (\mathbf{Y}_{S_1}, \mathbf{X}_{S_2})\} > \kappa, \\ & \min_{S_1 \subseteq \{j\}^c, S_2 \subseteq \{l\}^c} \{|\text{Corr}(Y_j, X_l \mid \mathbf{Z}_S)| : Y_i \text{ is not } d\text{-separated from } Y_j \mid \mathbf{Z}_S = (\mathbf{Y}_{S_1}, \mathbf{X}_{S_2})\} > \kappa, \end{aligned} \quad (26)$$

Then strong-faithfulness in (26) assumes 152 conditions for the correlations. By comparison, (17) requires the absolute values of five elements $V_{11}, V_{12}, V_{22}, V_{23}, V_{33}$ exceed $O(\sqrt{s \log(q)/n})$, which in turn requires the minimal absolute value of five correlations exceeds $O(\sqrt{s \log(q)/n})$,

- (i) $\text{Corr}(Y_1, X_1 \mid X_2, X_3)$,
- (ii) $\text{Corr}(Y_2, X_1 \mid X_2, X_3)$,
- (iii) $\text{Corr}(Y_2, X_2 \mid X_1, X_3)$,
- (iv) $\text{Corr}(Y_3, X_2 \mid X_1, X_3)$,
- (v) $\text{Corr}(Y_3, X_3 \mid X_1, X_2)$.

Note that $V_{13} \neq 0$ is not required because $Y_1 \rightarrow Y_3$ does not constitute an immediate parent-child relation. Importantly, (i)-(v) are required in (4), suggesting that strong-faithfulness is more stringent than (17).

Appendix B. Technical proofs

Proof of Proposition 1

Suppose that $\boldsymbol{\theta} = (\mathbf{U}, \mathbf{W}, \boldsymbol{\Sigma})$ and $\tilde{\boldsymbol{\theta}} = (\tilde{\mathbf{U}}, \tilde{\mathbf{W}}, \tilde{\boldsymbol{\Sigma}})$ render the same distribution of (\mathbf{Y}, \mathbf{X}) . We will prove that $\boldsymbol{\theta} = \tilde{\boldsymbol{\theta}}$.

Denote by $G(\boldsymbol{\theta})$ and $G(\tilde{\boldsymbol{\theta}})$ the DAGs corresponding to $\boldsymbol{\theta}$ and $\tilde{\boldsymbol{\theta}}$, respectively. First, consider $G(\boldsymbol{\theta})$. Without loss of generality, assume Y_1 is a leaf node. By Assumption 1C, there exists an instrumental intervention with respect to $G(\boldsymbol{\theta})$, say X_1 . Then,

$$\text{Cov}(Y_j, X_1 \mid \mathbf{X}_{\{2, \dots, q\}}) = 0, \quad j = 2, \dots, p, \quad (27)$$

$$\text{Cov}(Y_1, X_1 \mid \mathbf{Y}_S, \mathbf{X}_{\{2, \dots, q\}}) \neq 0, \quad \text{for any } S \subseteq \{2, \dots, p\}. \quad (28)$$

By the local Markov property (Spirtes et al., 2000), (28) implies that $X_1 \rightarrow Y_1$ in $G(\tilde{\boldsymbol{\theta}})$. Now, suppose Y_1 is not a leaf node in $G(\tilde{\boldsymbol{\theta}})$ and assume, without loss of generality, that $Y_1 \Rightarrow Y_2$. Then we have $\text{Cov}(Y_2, X_1 \mid \mathbf{X}_{\{2, \dots, q\}}) = 0$ but $X_1 \rightarrow Y_1$ and $Y_1 \Rightarrow Y_2$, which contradicts to Assumption 1B. This implies that if Y_1 is a leaf node in $G(\boldsymbol{\theta})$ then it must be also a leaf node in $G(\tilde{\boldsymbol{\theta}})$. Additionally, Y_1 has the same interventions in $G(\boldsymbol{\theta})$ and $G(\tilde{\boldsymbol{\theta}})$.

The forgoing argument is applied to other nodes sequentially. First, we remove Y_1 with any directed edges to Y_1 , which does not alter the joint distribution of $(\mathbf{Y}_{\{2, \dots, p\}}, \mathbf{X})$ and the subgraph of nodes Y_2, \dots, Y_p . By induction, we can always remove the leaves in $G(\boldsymbol{\theta})$ until it is empty, leading to $G(\boldsymbol{\theta}) = G(\tilde{\boldsymbol{\theta}})$. Finally, $\boldsymbol{\theta} = \tilde{\boldsymbol{\theta}}$ because they correspond to the same structural equations as $G(\boldsymbol{\theta}) = G(\tilde{\boldsymbol{\theta}})$ and these model parameters or regression coefficients are uniquely determined by Assumption 1A (Shojaie and Michailidis, 2010). This completes the proof.

Proof of Proposition 2

PROOF OF (A)

Note that the maximum length of a DAG is at most $p - 1$. Then it can be verified that its adjacency matrix \mathbf{U} is nilpotent in that $\mathbf{U}^p = \mathbf{0}$. An application of the matrix series expansion yields that $(\mathbf{I} - \mathbf{U})^{-1} = \mathbf{I} + \mathbf{U} + \dots + \mathbf{U}^{p-1}$. Using the fact that $\mathbf{V} = \mathbf{W}(\mathbf{I} - \mathbf{U})^{-1}$ from (13), we have that, for any $1 \leq l, j \leq p$,

$$V_{lj} = \sum_{i=1}^p W_{li}(I_{ij} + U_{ij} + \dots + (\mathbf{U}^{p-1})_{ij}),$$

where U_{ij} is the ij th entry of \mathbf{U} . If $V_{lj} \neq 0$, then there exists an i^0 such that $W_{li^0} \neq 0$ and $(\mathbf{U}^k)_{i^0j} \neq 0$ for some $0 \leq k \leq p - 1$. If $k = 0$, then we must have $i^0 = j$, and $X_l \rightarrow Y_j$. If $k > 0$, then $X_l \rightarrow Y_{i^0}$ and Y_{i^0} is an ancestor of Y_j .

PROOF OF (B)

First, for any leaf node variable Y_j , by Assumption 1, there exists an instrument $X_l \rightarrow Y_j$. If $\|\mathbf{V}_{l\bullet}\|_0 > 1$, then $V_{lj'} \neq 0$ for some $j' \neq j$. Then Y_j must be an ancestor of $Y_{j'}$, which contradicts the fact that Y_j is a leaf node variable.

Conversely, suppose that $V_{lj} \neq 0$ and $\|\mathbf{V}_{l\bullet}\|_0 = 1$. If Y_j is not a leaf node variable, then there exists an index $Y_{j'}$ such that $Y_j \Rightarrow Y_{j'}$, that is $U_{jj'} \neq 0$ and $(\mathbf{U}^k)_{jj'} = 0$ for $k > 1$. Then $V_{lj'} = W_{lj}U_{jj'} \neq 0$, which contradicts that $\|\mathbf{V}_{l\bullet}\|_0 = 1$. This completes the proof.

Proof of Theorem 8

Our proof proceeds in two steps:

- (A) Show that $\{l : |V_{lj}^0| \geq \tau^*\} \subseteq \text{supp}(\widehat{\mathbf{V}}_{\bullet j}) \subseteq \{l : V_{lj}^0 \neq 0\}$ almost surely; $j = 1, \dots, p$.
- (B) Show that $\widehat{\mathcal{S}} = \mathcal{S}^0$ if $\widehat{\mathbf{V}}$ satisfies the property in (A).

PROOF OF (A)

Denote $S_j^* = \{l : |V_{lj}^0| \geq \tau^*\}$ and $S_j = \{l : V_{lj} \neq 0\}$. We shall prove that $S_j^* \setminus \text{supp}(\widehat{\mathbf{V}}_{\bullet j}^{[T]}) = \emptyset$ and $\text{supp}(\widehat{\mathbf{V}}_{\bullet j}^{[T]}) \setminus S_j = \emptyset$; $j = 1, \dots, p$, with a high probability, where T is the iteration index at termination of Algorithm 2.

Let $S_j^{[t]} = \{l : |\widetilde{V}_{lj}^{[t]}| \geq \tau\}$ be the estimated support of penalized solution at the t -th iteration of Algorithm 2. For the penalized solution, define the false negative selection set $\text{FN}_j^{[t]} = S_j^* \setminus S_j^{[t]}$ and the false positive selection set $\text{FP}_j^{[t]} = S_j^{[t]} \setminus S_j$; $t = 0, 1, \dots, T$. Consider a “good” event $\mathcal{E}_j = \{\|\mathbb{X}^\top \widehat{\boldsymbol{\xi}}_j / n\|_\infty \leq 0.5\gamma\tau\} \cap \{\|\widehat{\mathbf{V}}_{\bullet j}^o - \mathbf{V}_{\bullet j}^0\|_\infty \leq 0.5\tau\}$, where $\widehat{\boldsymbol{\xi}}_j = \mathbb{Y}_j - \mathbb{X}\widehat{\mathbf{V}}_{\bullet j}^o$ is the residual of the least squares estimate $\widehat{\mathbf{V}}_{\bullet j}^o$ such that $S_j = \{l : \widehat{V}_{lj}^o \neq 0\}$; $j = 1, \dots, p$. We shall show that $\text{FN}_j^{[t]}$ and $\text{FP}_j^{[t]}$ are eventually empty sets on event \mathcal{E}_j which has a probability tending to one.

Towards this end, we first show that if $|S_j \cup S_j^{[t-1]}| \leq 2K_{\max}^0$ on \mathcal{E}_j for $t \geq 1$, then $|S_j \cup S_j^{[t]}| \leq 2K_{\max}^0$, to be used in Assumption 2. Now suppose $|S_j \cup S_j^{[t-1]}| \leq 2K_{\max}^0$ on \mathcal{E}_j

for $t \geq 1$. By the optimality condition of (14),

$$(\widehat{\mathbf{V}}_{\bullet j}^o - \widetilde{\mathbf{V}}_{\bullet j}^{[t]})^\top \left(-\mathbb{X}^\top (\mathbb{Y}_j - \mathbb{X} \widetilde{\mathbf{V}}_{\bullet j}^{[t]})/n + \gamma\tau \nabla \|(\widetilde{\mathbf{V}}_{\bullet j}^{[t]})_{(S_j^{[t-1]})^c}\|_1 \right) \geq 0. \quad (29)$$

Rearranging the inequality yields that

$$\begin{aligned} \|\mathbb{X}(\widetilde{\mathbf{V}}_{\bullet j}^{[t]} - \widehat{\mathbf{V}}_{\bullet j}^o)\|_2^2/n &\leq (\widetilde{\mathbf{V}}_{\bullet j}^{[t]} - \widehat{\mathbf{V}}_{\bullet j}^o)^\top \left(\mathbb{X}^\top \widehat{\boldsymbol{\xi}}_j/n - \gamma\tau \nabla \|(\widetilde{\mathbf{V}}_{\bullet j}^{[t]})_{(S_j^{[t-1]})^c}\|_1 \right) \\ &= (\widetilde{\mathbf{V}}_{\bullet j}^{[t]} - \widehat{\mathbf{V}}_{\bullet j}^o)_{S_j \setminus S_j^{[t-1]}}^\top \left(\mathbb{X}^\top \widehat{\boldsymbol{\xi}}_j/n - \gamma\tau \nabla \|(\widetilde{\mathbf{V}}_{\bullet j}^{[t]})_{(S_j^{[t-1]})^c}\|_1 \right)_{S_j \setminus S_j^{[t-1]}} \\ &\quad + (\widetilde{\mathbf{V}}_{\bullet j}^{[t]} - \widehat{\mathbf{V}}_{\bullet j}^o)_{(S_j \cup S_j^{[t-1]})^c}^\top \left(\mathbb{X}^\top \widehat{\boldsymbol{\xi}}_j/n - \gamma\tau \nabla \|(\widetilde{\mathbf{V}}_{\bullet j}^{[t]})_{(S_j^{[t-1]})^c}\|_1 \right)_{(S_j \cup S_j^{[t-1]})^c}. \end{aligned} \quad (30)$$

It follows from the fact that that $(\mathbb{X}^\top \widehat{\boldsymbol{\xi}}_j/n - \gamma\tau \nabla \|(\widetilde{\mathbf{V}}_{\bullet j}^{[t]})_{(S_j^{[t-1]})^c}\|_1)_{S_j^{[t-1]}} = \mathbf{0}_{S_j^{[t-1]}}$ and $(\widetilde{\mathbf{V}}_{\bullet j}^{[t]} - \widehat{\mathbf{V}}_{\bullet j}^o)_{(S_j \cup S_j^{[t-1]})^c}^\top (\nabla \|(\widetilde{\mathbf{V}}_{\bullet j}^{[t]})_{(S_j^{[t-1]})^c}\|_1)_{(S_j \cup S_j^{[t-1]})^c} = \|(\widetilde{\mathbf{V}}_{\bullet j}^{[t]} - \widehat{\mathbf{V}}_{\bullet j}^o)_{(S_j \cup S_j^{[t-1]})^c}\|_1$. Then (30) is no greater than

$$\|(\widetilde{\mathbf{V}}_{\bullet j}^{[t]} - \widehat{\mathbf{V}}_{\bullet j}^o)_{S_j \setminus S_j^{[t-1]}}\|_1 \left(\|\mathbb{X}^\top \widehat{\boldsymbol{\xi}}_j/n\|_\infty + \gamma\tau \right) + \|(\widetilde{\mathbf{V}}_{\bullet j}^{[t]} - \widehat{\mathbf{V}}_{\bullet j}^o)_{(S_j \cup S_j^{[t-1]})^c}\|_1 \left(\|\mathbb{X}^\top \widehat{\boldsymbol{\xi}}_j/n\|_\infty - \gamma\tau \right). \quad (31)$$

Note that $\|\mathbb{X}(\widetilde{\mathbf{V}}_{\bullet j}^{[t]} - \widehat{\mathbf{V}}_{\bullet j}^o)\|_2^2/n \geq 0$. Rearranging the inequality yields

$$(\gamma\tau - \|\mathbb{X}^\top \widehat{\boldsymbol{\xi}}_j/n\|_\infty) \|(\widetilde{\mathbf{V}}_{\bullet j}^{[t]} - \widehat{\mathbf{V}}_{\bullet j}^o)_{(S_j \cup S_j^{[t-1]})^c}\|_1 \leq (\|\mathbb{X}^\top \widehat{\boldsymbol{\xi}}_j/n\|_\infty + \gamma\tau) \|(\widetilde{\mathbf{V}}_{\bullet j}^{[t]} - \widehat{\mathbf{V}}_{\bullet j}^o)_{S_j \setminus S_j^{[t-1]}}\|_1.$$

On event \mathcal{E}_j , $\|\mathbb{X}^\top \widehat{\boldsymbol{\xi}}_j/n\|_\infty \leq \gamma\tau/2$, implying that $\|(\widetilde{\mathbf{V}}_{\bullet j}^{[t]} - \widehat{\mathbf{V}}_{\bullet j}^o)_{(S_j \cup S_j^{[t-1]})^c}\|_1 \leq 3\|(\widetilde{\mathbf{V}}_{\bullet j}^{[t]} - \widehat{\mathbf{V}}_{\bullet j}^o)_{S_j \setminus S_j^{[t-1]}}\|_1 \leq 3\|(\widetilde{\mathbf{V}}_{\bullet j}^{[t]} - \widehat{\mathbf{V}}_{\bullet j}^o)_{S_j \cup S_j^{[t-1]}}\|_1$. Note that $|S_j \cup S_j^{[t-1]}| \leq 2K_{\max}^0$. By the restricted eigenvalue condition in Assumption 2 and (31),

$$\begin{aligned} \Lambda_{\min} \|\widetilde{\mathbf{V}}_{\bullet j}^{[t]} - \widehat{\mathbf{V}}_{\bullet j}^o\|_2^2 &\leq \|\mathbb{X}(\widetilde{\mathbf{V}}_{\bullet j}^{[t]} - \widehat{\mathbf{V}}_{\bullet j}^o)\|_2^2/n \\ &\leq \left(\|\mathbb{X}^\top \widehat{\boldsymbol{\xi}}_j/n\|_\infty + \gamma\tau \right) \|(\widetilde{\mathbf{V}}_{\bullet j}^{[t]} - \widehat{\mathbf{V}}_{\bullet j}^o)_{S_j \setminus S_j^{[t-1]}}\|_1 + \left(\|\mathbb{X}^\top \widehat{\boldsymbol{\xi}}_j/n\|_\infty - \gamma\tau \right) \|(\widetilde{\mathbf{V}}_{\bullet j}^{[t]} - \widehat{\mathbf{V}}_{\bullet j}^o)_{(S_j \cup S_j^{[t-1]})^c}\|_1 \\ &\leq \left(\|\mathbb{X}^\top \widehat{\boldsymbol{\xi}}_j/n\|_\infty + \gamma\tau \right) \|(\widetilde{\mathbf{V}}_{\bullet j}^{[t]} - \widehat{\mathbf{V}}_{\bullet j}^o)_{S_j \setminus S_j^{[t-1]}}\|_1. \end{aligned} \quad (32)$$

By the Cauchy-Schwarz inequality, $\|(\widetilde{\mathbf{V}}_{\bullet j}^{[t]} - \widehat{\mathbf{V}}_{\bullet j}^o)_{S_j \setminus S_j^{[t-1]}}\|_1 \leq \sqrt{|S_j \setminus S_j^{[t-1]}|} \|\widetilde{\mathbf{V}}_{\bullet j}^{[t]} - \widehat{\mathbf{V}}_{\bullet j}^o\|_2$. Thus, $\Lambda_{\min} \|\widetilde{\mathbf{V}}_{\bullet j}^{[t]} - \widehat{\mathbf{V}}_{\bullet j}^o\|_2^2 \leq 1.5\gamma\tau \sqrt{K_{\max}^0}$, since $|S_j \setminus S_j^{[t-1]}| \leq |S_j| \leq K_{\max}^0$ and $\|\mathbb{X}^\top \widehat{\boldsymbol{\xi}}_j/n\|_\infty \leq 0.5\gamma\tau$. By the condition (1) of Theorem 8, $\gamma \leq \Lambda_{\min}/6$ and $\|\widetilde{\mathbf{V}}_{\bullet j}^{[t]} - \widehat{\mathbf{V}}_{\bullet j}^o\|_2/\tau \leq \sqrt{K_{\max}^0}$. On the other hand, for any $l \in \text{FP}_j^{[t]} = S_j^{[t]} \setminus S_j$, we have $|\widetilde{V}_{lj}^{[t]} - \widehat{V}_{lj}^o| = |\widetilde{V}_{lj}^{[t]}| > \tau$. Thus, $\sqrt{|\text{FP}_j^{[t]}|} \leq \|\widetilde{\mathbf{V}}_{\bullet j}^{[t]} - \widehat{\mathbf{V}}_{\bullet j}^o\|_2/\tau \leq \sqrt{K_{\max}^0}$. Consequently, $|S_j \cup S_j^{[t]}| = |S_j| + |\text{FP}_j^{[t]}| \leq 2K_{\max}^0$ on \mathcal{E}_j for $t \geq 1$.

Next, we estimate the number of iterations required for termination. We shall show that $|\text{FN}_j^{[t]}| < 1$ and $|\text{FP}_j^{[t]}| < 1$ eventually.

Suppose $|\text{FN}_j^{[t]}| \geq 1$. For any $l \in \text{FN}_j^{[t]}$, by Assumption 6, $|\tilde{V}_{lj}^{[t]} - \hat{V}_{lj}^o| \geq |\tilde{V}_{lj}^{[t]} - V_{lj}^0| - |\hat{V}_{lj}^o - V_{lj}^0| \geq \tau^* - 1.5\tau$, so $\|\tilde{\mathbf{V}}_{\bullet j}^{[t]} - \hat{\mathbf{V}}_{\bullet j}^o\|_2^2 \geq |\text{FN}_j^{[t]}|(\tau^* - 1.5\tau)^2$, or $\sqrt{|\text{FN}_j^{[t]}|} \leq \|\tilde{\mathbf{V}}_{\bullet j}^{[t]} - \hat{\mathbf{V}}_{\bullet j}^o\|_2 / (\tau^* - 1.5\tau)$. By (32) and the Cauchy-Schwarz inequality, we have $\Lambda_{\min} \|\tilde{\mathbf{V}}_{\bullet j}^{[t]} - \hat{\mathbf{V}}_{\bullet j}^o\|_2 \leq 1.5\gamma\tau \left(\sqrt{|\text{FN}_j^{[t-1]}|} + \sqrt{|S_j \setminus (S_j^{[t-1]} \cup S_j^*)|} \right)$. By conditions (1) and (2) for (τ, γ) in Theorem 8, we have

$$\begin{aligned} \sqrt{|\text{FN}_j^{[t]}|} &\leq \frac{\|\tilde{\mathbf{V}}_{\bullet j}^{[t]} - \hat{\mathbf{V}}_{\bullet j}^o\|_2}{\tau^* - 1.5\tau} \leq \frac{1.5\gamma\tau}{\Lambda_{\min}(\tau^* - 1.5\tau)} \left(\sqrt{|\text{FN}_j^{[t-1]}|} + \sqrt{K_j^0 - K_j^*} \right) \\ &\leq 0.25\sqrt{|\text{FN}_j^{[t-1]}|} + 0.25. \end{aligned}$$

Hence, $\sqrt{|\text{FN}_j^{[t]}|} \leq (1/4)^t \sqrt{|S_j^*|} + 1/3$. In particular, for $t \geq 1 + \lceil \log K_j^* / \log 4 \rceil$, $|\text{FN}_j^{[t]}| < 1$ implying that $\text{FN}_j^{[t]} = \emptyset$.

Similarly, suppose $|\text{FP}_j^{[t]}| \geq 1$. Then $\|\tilde{\mathbf{V}}_{\bullet j}^{[t]} - \hat{\mathbf{V}}_{\bullet j}^o\|_2^2 \geq |\text{FP}_j^{[t]}|\tau^2$. By conditions (1) and (2) for (τ, γ) in Theorem 8, we have

$$\sqrt{|\text{FP}_j^{[t]}|} \leq \frac{\|\tilde{\mathbf{V}}_{\bullet j}^{[t]} - \hat{\mathbf{V}}_{\bullet j}^o\|_2}{\tau} \leq \frac{1.5\gamma}{\Lambda_{\min}} \left(\sqrt{|\text{FN}_j^{[t-1]}|} + \sqrt{K_j^0 - K_j^*} \right) \leq 0.25\sqrt{|\text{FN}_j^{[t-1]}|} + 0.25.$$

Thus, $\sqrt{|\text{FP}_j^{[t]}|} \leq (1/4)^t \sqrt{|S_j^*|} + 1/3$ and $\text{FP}_j^{[t]} = \emptyset$ for $t \geq 1 + \lceil \log K_j^* / \log 4 \rceil$.

Let $T = 1 + \lceil \log K_j^* / \log 4 \rceil$. Then $\text{FN}_j^{[T]} = \text{FP}_j^{[T]} = \emptyset$ on event \mathcal{E}_j . Under condition (3), we have $S_j^* \subseteq \text{supp}(\hat{\mathbf{V}}_{\bullet j}) \subseteq \text{supp}(\hat{\mathbf{V}}_{\bullet j}^{[T]}) \subseteq S_j$. It remains to bound $P(\bigcup_{j=1}^p \mathcal{E}_j^c)$. By the Borell-TIS inequality,

$$\begin{aligned} P(\|\mathbb{X}^\top \hat{\boldsymbol{\xi}}_j / n\|_\infty > 0.5\gamma\tau) &= P(\|\mathbb{X}^\top (\mathbf{I} - \mathbf{P}_{S_j}) \boldsymbol{\xi}_j / n\|_\infty > 0.5\gamma\tau) \leq 2q \exp \left(-\frac{\gamma_j^2 \tau_j^2 n}{8c_2^2 \Omega_{jj}} \right), \\ P(\|\hat{\mathbf{V}}_{\bullet j}^o - \mathbf{V}_{\bullet j}^0\|_\infty > 0.5\tau) &= P(\|(\mathbb{X}_{S_j}^\top \mathbb{X}_{S_j})^{-1} \mathbb{X}_{S_j}^\top \boldsymbol{\xi}_j\|_\infty > 0.5\tau) \leq 2K_{\max}^0 \exp \left(-\frac{\tau_j^2 n}{8c_2^2 \Omega_{jj}} \right), \end{aligned}$$

where $\boldsymbol{\xi}_j = ((\varepsilon_V)_{1j}, \dots, (\varepsilon_V)_{nj})^\top \in \mathbb{R}^n$. Then under conditions (1) and (2) for (τ, γ) in Theorem 8,

$$P \left(\forall j : S_j^* \subseteq \text{supp}(\hat{\mathbf{V}}_{\bullet j}) \subseteq S_j \right) \geq 1 - P \left(\bigcup_{j=1}^p \mathcal{E}_j^c \right) \geq 1 - 4q^{-2}.$$

By Borel-Cantelli lemma, $S_j^* \subseteq \text{supp}(\hat{\mathbf{V}}_{\bullet j}) \subseteq S_j$; $j = 1, \dots, p$ almost surely as $n, p, q \rightarrow \infty$.

PROOF OF (B)

Assume $\widehat{\mathbf{V}}$ satisfies the properties in (A). Then Proposition 2 also holds true for $\widehat{\mathbf{V}}$. We shall prove (B) by induction.

For $t = 1$, by Proposition 2, Algorithm 3 can identify the set of leaf nodes $\mathbf{Y}_{B^{[1]}}$ with their corresponding instruments $\mathbf{X}_{A^{[1]}}$ of the DAG $G^0 = G^{[1]}$, where $A^{[1]} = \{l : l = \arg \min_{\|\widehat{\mathbf{V}}_{l\bullet}^{[1]}\|_0 \neq 0} \|\widehat{\mathbf{V}}_{l\bullet}^{[1]}\|_0\}$. Moreover, $C^{[1]} = \{m \neq \arg \min_{\|\widehat{\mathbf{V}}_{m\bullet}^{[1]}\|_0 \neq 0} \|\widehat{\mathbf{V}}_{m\bullet}^{[1]}\|_0 : \widehat{\mathbf{V}}_{mj}^{[1]} \neq 0\}$ collects all leaf-noninstruments. In model (1), after removing $(\mathbf{X}_{A^{[1]}}, \mathbf{Y}_{B^{[1]}})$, the local Markov property among $(\mathbf{X}_{\setminus A^{[1]}}, \mathbf{Y}_{\setminus B^{[1]}})$ remain intact. Hence, the joint distribution of $(\mathbf{X}_{\setminus A^{[1]}}, \mathbf{Y}_{\setminus B^{[1]}})$ is associated with the subgraph $G^{[2]}$ by removing the nodes in $A^{[1]}$, $B^{[1]}$, and all the corresponding edges.

Assume for iterations $1, \dots, t-1$, Algorithm 3 correctly identifies the leaf nodes and the corresponding interventions. Then at t th iteration, Algorithm 3 identifies the leaf nodes $\mathbf{Y}_{B^{[t]}}$ with their instrumental interventions $\mathbf{X}_{A^{[t]}}$ in subgraph $G^{[t]}$. By Proposition 2 and Assumption 1B, for a leaf node $j \in B^{[t]}$, $Y_j \Rightarrow Y_k$ if and only if $k \in B^{[t-1]}$ is removed in last consecutive iteration, and $V_k \neq 0$ for all instrumental variables X_l on Y_j in $G^{[t]}$. Also, $C^{[t]}$ collects all non-instruments on leaf nodes of $G^{[t]}$. Again, removing $(\mathbf{X}_{A^{[t]}}, \mathbf{Y}_{B^{[t]}})$ induces subgraph $G^{[t+1]}$.

Consequently, after removing all nodes, Algorithm 3 recovers all immediate parent-child relations. Step 7 reconstructs the ancestor and relevant intervention relations of the true DAG. Therefore, Algorithm 3 recovers $\widehat{\mathcal{S}} = \mathcal{S}^0$ and $\widehat{D} = D^0$ almost surely as $n, p, q \rightarrow \infty$. This completes the proof of (B).

Proof of Theorem 3

Our proof proceeds in three steps:

- (A) Show that $\{l : \widehat{V}_{lj} \neq 0\} = \{l : V_{lj}^0 \neq 0\}$ almost surely; $j = 1, \dots, p$.
- (B) Show that $\widehat{\mathcal{S}} = \mathcal{S}^0$ if $\widehat{\mathbf{V}}$ satisfies the property in (A).
- (C) Show that Algorithm 2 converges to the global minimizer $\widehat{\mathbf{V}}_{\bullet j}$ almost surely.

PROOF OF (A) AND (B)

Note that if $K_j^* = K_j^0$ in Assumption 6, then Assumption 6 is reduced to Assumption 4. Then (A) and (B) are implied by Theorem 8.

PROOF OF (C)

By (A) and (B), we have $S_j^* = S_j$ and $\widehat{\mathbf{V}}_{\bullet j} = \widehat{\mathbf{V}}_{\bullet j}^o$; $j = 1, \dots, p$, almost surely. It remains to show that $\widehat{\mathbf{V}}_{\bullet j}^o$; $j = 1, \dots, p$ is a global minimizer of (14) with a high probability. Note that Assumption 2 and Assumption 4 imply the degree of separation condition (Shen et al., 2013). By Theorem 2 of Shen et al. (2013),

$$P(\widehat{\mathbf{V}}_{\bullet j}^o \text{ is not a global minimizer of (14)}) \leq 3 \exp(-2 \log p).$$

implying that $\widehat{\mathbf{V}}_{\bullet j}^o$ is a global minimizer of (14) almost surely, as $n, p, q \rightarrow \infty$. This completes the proof.

Lemma 9 *Let*

$$T_j = \frac{\mathbf{e}_j^\top (\mathbf{P}_{A_j^0} - \mathbf{P}_{B_j^0}) \mathbf{e}_j}{\mathbf{e}_j^\top (\mathbf{I} - \mathbf{P}_{A_j^0}) \mathbf{e}_j / (n - |A_j^0|)}, \quad T_j^* = \frac{(\mathbf{e}_j^*)^\top (\mathbf{P}_{A_j^0} - \mathbf{P}_{B_j^0}) \mathbf{e}_j^*}{(\mathbf{e}_j^*)^\top (\mathbf{I} - \mathbf{P}_{A_j^0}) \mathbf{e}_j^* / (n - |A_j^0|)}, \quad (33)$$

where $A_j^0 = \text{AN}(j) \cup \text{INT}(j)$, $B_j^0 = A_j^0 \setminus \{k : (k, j) \in D\} \subseteq A_j^0$. Then (T_1, \dots, T_p) are independent and (T_1^*, \dots, T_p^*) are conditionally independent given \mathcal{Z} . Moreover, $T_j / (|A_j^0| - |B_j^0|) \stackrel{d}{=} T_j^* / (|A_j^0| - |B_j^0|) \mid \mathcal{Z} \sim F_{|A_j^0| - |B_j^0|, n - |A_j^0|}$; $j = 1, \dots, p$, where F_{d_1, d_2} denotes the F -distribution with d_1 and d_2 degrees of freedom.

Proof of Lemma 9

Let $\mathbb{Z} = (\mathbb{Y}, \mathbb{X})$ as in (8). Given data submatrix $\mathbb{Z}_{A_j^0}$, $\mathbf{e}_j^\top (\mathbf{P}_{A_j^0} - \mathbf{P}_{B_j^0}) \mathbf{e}_j / \sigma_j^2 \mid \mathbb{Z}_{A_j^0} \sim \chi_{|A_j^0| - |B_j^0|}^2$ and $\mathbf{e}_j^\top (\mathbf{I} - \mathbf{P}_{A_j^0}) \mathbf{e}_j / \sigma_j^2 \mid \mathbb{Z}_{A_j^0} \sim \chi_{n - |A_j^0|}^2$ are independent, because $\mathbf{P}_{A_j^0} - \mathbf{P}_{B_j^0}$ and $\mathbf{I} - \mathbf{P}_{A_j^0}$ are orthonormal projection matrices, $\mathbf{e}_j \mid \mathbb{Z}_{A_j^0} \sim N(\mathbf{0}, \sigma_j^2 \mathbf{I}_n)$, and $(\mathbf{P}_{A_j^0} - \mathbf{P}_{B_j^0})(\mathbf{I} - \mathbf{P}_{A_j^0}) = \mathbf{0}$. Then, for any $t \in \mathbb{R}$, the characteristic function $E \exp(itT_j / (|A_j^0| - |B_j^0|))$ can be written as

$$E \left(E \left(\exp(itT_j / (|A_j^0| - |B_j^0|)) \mid \mathbb{Z}_{A_j^0} \right) \right) = E \psi_{|A_j^0| - |B_j^0|, n - |A_j^0|}(t) = \psi_{|A_j^0| - |B_j^0|, n - |A_j^0|}(t),$$

where $\psi_{|A_j^0| - |B_j^0|, n - |A_j^0|}$ is the characteristic function of F -distribution with degrees of freedom $|A_j^0| - |B_j^0|$ and $n - |A_j^0|$. Hence, $T_j / (|A_j^0| - |B_j^0|) \sim F_{|A_j^0| - |B_j^0|, n - |A_j^0|}$. Similarly, $T_j^* / (|A_j^0| - |B_j^0|) \sim F_{|A_j^0| - |B_j^0|, n - |A_j^0|}$; $j = 1, \dots, p$.

Next, we prove independence for T and T^* via the peeling strategy. Let $\mathbf{t} = (t_1, \dots, t_p)^\top \in \mathbb{R}^p$. Let j_0 be a leaf node of the graph G^0 . Then $\mathbf{T}_{-j_0} \mid \mathbb{Y}_{-j_0}, \mathbb{X}$ is deterministic, where \mathbf{T}_{-j} is the subvector of \mathbf{T} with the j th component removed. The characteristic function of $\mathbf{t}^\top \mathbf{T}$ is

$$\begin{aligned} E \exp(i\mathbf{t}^\top \mathbf{T}) &= E \left(E \left(\exp(it_{j_0} T_{j_0}) \mid \mathbb{Y}_{-j_0}, \mathbb{X} \right) \exp(i\mathbf{t}_{-j_0}^\top \mathbf{T}_{-j_0}) \right) \\ &= \psi_{|A_{j_0}^0| - |B_{j_0}^0|, n - |A_{j_0}^0|}(t_{j_0}) E \exp(i\mathbf{t}_{-j_0}^\top \mathbf{T}_{-j_0}), \end{aligned} \quad (34)$$

where $\psi_{|A_{j_0}^0| - |B_{j_0}^0|, n - |A_{j_0}^0|}$ is the characteristic function of the F -distribution with degrees of freedom $(|A_{j_0}^0| - |B_{j_0}^0|, n - |A_{j_0}^0|)$. Next, let j_1 be a leaf node of the graph G^1 and apply the law of iterated expectation again, where G^1 is the subgraph of G^0 without node j_0 . Repeat this procedure and after p steps $E \exp(i\mathbf{t}^\top \mathbf{T}) = \prod_{j=1}^p \psi_{|A_j^0| - |B_j^0|, n - |A_j^0|}(t_j)$, which implies (T_1, \dots, T_p) are independent. Similarly, \mathbf{T}^* also has independent components given \mathcal{Z} and has the same distribution as \mathbf{T} . This completes the proof.

Proof of Theorem 4

PROOF OF (A)

Without loss of generality, assume M is sufficiently large. For any $x \in \mathbb{R}$,

$$\begin{aligned} |P(\text{Lr} \leq x) - P(\text{Lr}(S^0, \widehat{\Sigma}) \leq x)| &\leq E|I(\text{Lr} \leq x) - I(\text{Lr}(S^0, \widehat{\Sigma}) \leq x)| \\ &= E|I(\text{Lr} \leq x, \widehat{S} \neq S^0) + I(\text{Lr}(S^0, \widehat{\Sigma}) \leq x)(I(\widehat{S} = S^0) - 1)| \leq 2P(\widehat{S} \neq S^0). \end{aligned} \quad (35)$$

From (9), $\text{Lr}^*(S^0, \widehat{\Sigma}^*) = \sum_{j:(i,j) \in D} T_j^*$. By Lemma 9, $P(\text{Lr}(S^0, \widehat{\Sigma}) \leq x) = P(\text{Lr}^*(S^0, \widehat{\Sigma}^*) \leq x \mid \mathcal{Z})$. Note that $\text{Lr}^* = \text{Lr}^*(\widehat{S}^*, \widehat{\Sigma}^*)$. Then for any $x \in \mathbb{R}$,

$$\begin{aligned} & |P(\text{Lr}^* \leq x \mid \mathcal{Z}) - P(\text{Lr}(S^0, \widehat{\Sigma}) \leq x)| \\ &= |P(\text{Lr}^* \leq x, \widehat{S}^* \neq S^0 \mid \mathcal{Z}) + P(\text{Lr}^*(S^0, \widehat{\Sigma}^*) \leq x, \widehat{S}^* = S^0 \mid \mathcal{Z}) - P(\text{Lr}^*(S^0, \widehat{\Sigma}^*) \leq x \mid \mathcal{Z})| \\ &\leq |P(\text{Lr}^* \leq x, \widehat{S}^* \neq S^0 \mid \mathcal{Z})| + |P(\text{Lr}^*(S^0, \widehat{\Sigma}^*) \leq x, \widehat{S}^* \neq S^0 \mid \mathcal{Z})| \leq 2P(\widehat{S}^* \neq S^0 \mid \mathcal{Z}). \end{aligned} \quad (36)$$

Since (35) and (36) hold uniformly in x , we have

$$\sup_{x \in \mathbb{R}} |P(\text{Lr} \leq x) - P(\text{Lr}^* \leq x \mid \mathcal{Z})| \leq 2P(\widehat{S} \neq S^0) + 2P(\widehat{S}^* \neq S^0 \mid \mathcal{Z}).$$

By Theorem 3, we have $P(\widehat{S} \neq S^0) \rightarrow 0$, which holds uniformly for all θ which satisfy the Assumptions 1C-5. For $P(\widehat{S}^* \neq S^0 \mid \mathcal{Z})$, note that the perturbation size δ satisfy $\delta^2 \leq \min_{1 \leq j \leq p} 0.5\sigma_j^{-2} \left(\frac{(\tau_j^*)^2 c_1^2 n}{90c_2^2(K_j^0 - K_j^* + 1) \log q} - \Omega_{jj} \right)$. For the perturbed data \mathcal{Z}^* , the error terms of (14) are rescaled with $\Omega_{jj} + \delta^2 \widehat{\sigma}_j^2$. Thus, it follows from Theorem 3 that $P(\widehat{S}^* \neq S^0) = EP(\widehat{S}^* \neq S^0 \mid \mathcal{Z}) \rightarrow 0$, which implies $P(\widehat{S}^* \neq S^0 \mid \mathcal{Z}) \xrightarrow{p} 0$ as $n, p, q \rightarrow \infty$ by the Markov inequality. Consequently, $\sup_{x \in \mathbb{R}} |P(\text{Lr} \leq x) - P(\text{Lr}^* \leq x \mid \mathcal{Z})| \rightarrow 0$. For $|D| = 0$, $P(\text{Lr} = 0) \rightarrow 1$, $P(\text{Lr}^* = 0 \mid \mathcal{Z}) \rightarrow 1$, and $P(\text{Pval} = 1) \rightarrow 1$. For $|D| > 0$, $P(\text{Lr}^* \geq \text{Lr} \mid \mathcal{Z}) \rightarrow \text{Unif}(0, 1)$ and $P(\text{Pval} < \alpha) \rightarrow \alpha$. This completes the proof of (A).

PROOF OF (B)

Let $\text{Pval}_k = M^{-1} \sum_{m=1}^M I(\text{Lr}_{k,m}^* \geq \text{Lr})$, the p-value of sub-hypothesis $H_{0,k}$. For $|D| < |F|$, there exists some edge $(i_k, j_k) \in F$ but $(i_k, j_k) \notin D$. Then by (A), $P(\text{Pval} = \text{Pval}_k = 1) \rightarrow 1$. For $|D| = |F|$, note that as $n, p, q, M \rightarrow \infty$,

$$P(\text{Pval} < \alpha) = P(\text{Pval}_1 < \alpha, \dots, \text{Pval}_{|F|} < \alpha) \leq P(\text{Pval}_1 < \alpha) \rightarrow \alpha.$$

Now, define a sequence \mathbf{U}_F^r ; $r = 1, 2, \dots$ such that $\mathbf{U}_{(i_1, j_1)}^r = 0$ and $\min_{k=2}^{|F|} |\mathbf{U}_{(i_k, j_k)}^r| \geq c > 0$. Note that \mathbf{U}_F^r ; $r = 1, 2, \dots$ satisfies H_0 and $\text{Pval}_k \xrightarrow{p} 0$ as $r \rightarrow \infty$ by Proposition 6. Hence,

$$\limsup_{\substack{n, p, q \rightarrow \infty \\ \mathbf{U}_F^r \text{ satisfies } H_0}} P_{\theta_r}(\text{Pval} < \alpha) \geq \sup_r \lim_{n, p, q \rightarrow \infty} P_{\theta_r}(\text{Pval} < \alpha) = \alpha.$$

This completes the proof.

Proof of Proposition 5

Since $P(\hat{S} = S^0) \rightarrow 1$, it suffices to consider $\text{Lr}(S^0, \hat{\Sigma})$. For $|D| = 0$, we have $P(\text{Lr} = 0) \rightarrow 1$. Now, assume $|D| > 0$. Then

$$\begin{aligned} 2\text{Lr}(S^0, \hat{\Sigma}) &= \sum_{\{j: \exists(k,j) \in F\}} \frac{\mathbf{e}_j^\top (\mathbf{P}_{A_j^0} - \mathbf{P}_{B_j^0}) \mathbf{e}_j}{\sigma_j^2} + \sum_{\{j: \exists(k,j) \in F\}} \left(\frac{\sigma_j^2}{\hat{\sigma}_j^2} - 1 \right) \frac{\mathbf{e}_j^\top (\mathbf{P}_{A_j^0} - \mathbf{P}_{B_j^0}) \mathbf{e}_j}{\sigma_j^2} \\ &= \underbrace{\sum_{\{j: \exists(k,j) \in D\}} \frac{\mathbf{e}_j^\top (\mathbf{P}_{A_j^0} - \mathbf{P}_{B_j^0}) \mathbf{e}_j}{\sigma_j^2}}_{R_1} + \underbrace{\sum_{\{j: \exists(k,j) \in D\}} \left(\frac{\sigma_j^2}{\hat{\sigma}_j^2} - 1 \right) \frac{\mathbf{e}_j^\top (\mathbf{P}_{A_j^0} - \mathbf{P}_{B_j^0}) \mathbf{e}_j}{\sigma_j^2}}_{R_2}. \end{aligned}$$

To derive the asymptotic distribution of R_1 , we apply the peeling strategy with law of iterated expectation as in the proof of Lemma 9. Then we have $\mathbf{e}_j^\top (\mathbf{P}_{A_j^0} - \mathbf{P}_{B_j^0}) \mathbf{e}_j / \sigma_j^2$; $j : (i, j) \in D$ are independent. Therefore, $R_1 \sim \chi_{|D|}^2$.

To bound R_2 , we apply Lemma 1 of (Laurent and Massart, 2000). By Assumption 5, we have

$$P \left(\max_{j: (i,j) \in D} \left| \frac{\hat{\sigma}_j^2}{\sigma_j^2} - 1 \right| \geq 4 \sqrt{\frac{\log |D|}{(1-\rho)n}} + 8 \frac{\log |D|}{(1-\rho)n} \right) \leq 2 \exp(-\log |D|).$$

Hence, $\max_{j: (i,j) \in D} \left| \frac{\hat{\sigma}_j^2}{\sigma_j^2} - 1 \right| \leq 8 \sqrt{\frac{\log |D|}{(1-\rho)n}}$ with probability tending one as $n, p \rightarrow \infty$. Thus

$$|R_2| \leq |R_1| \max_{j: (i,j) \in D} \left| \frac{\sigma_j^2}{\hat{\sigma}_j^2} - 1 \right| \leq O_p \left(|D| \sqrt{\frac{\log |D|}{n}} \right).$$

Consequently, as $n, p, q \rightarrow \infty$, if $|D| > 0$ is fixed, then $2\text{Lr} \xrightarrow{d} \chi_{|D|}^2$; if $|D| \rightarrow \infty$, then $(2|D|)^{-1/2}(2\text{Lr} - |D|) \xrightarrow{d} N(0, 1)$. This completes the proof.

Proof of Proposition 6

Let $\boldsymbol{\theta}^n = (\mathbf{U}^0 + \mathbf{H}, \mathbf{W}^0, \Sigma^0)$. Then

$$l(\boldsymbol{\theta}^n) - l(\boldsymbol{\theta}^0) = \sum_{j=1}^p \left(n^{1/2} \boldsymbol{\eta}_j^\top \boldsymbol{\Delta}_j - 2^{-1} n^{1/2} \boldsymbol{\Delta}_j \left(n^{-1} \mathbb{Y}_{A_j^0 \setminus B_j^0}^\top \mathbb{Y}_{A_j^0 \setminus B_j^0} \right) n^{1/2} \boldsymbol{\Delta}_j \right),$$

where $\boldsymbol{\eta}_j = n^{-1/2} \mathbb{Y}_{A_j^0 \setminus B_j^0}^\top \mathbf{e}_j \in \mathbb{R}^{|A_j^0 \setminus B_j^0|}$, and $\boldsymbol{\Delta}_j \in \mathbb{R}^{|A_j^0 \setminus B_j^0|}$ such that $\Delta_{ij} = H_{ij}$ for $i \in A_j^0 \setminus B_j^0$. For the likelihood ratio, it suffices to consider $\text{Lr}(S^0, \hat{\Sigma})$, since $P(\hat{S} = S^0) \rightarrow 1$. Under H_0 , we have $2\text{Lr} = \sum_{j: (i,j) \in D} T_j$. Note that $T_j = \sum_{r=1}^{|A_j^0 \setminus B_j^0|} (\mathbf{q}_{jr}^\top \mathbf{e}_j)^2 + o_p(1)$ by Proposition 5, where $\mathbf{P}_{A_j^0} - \mathbf{P}_{B_j^0} = \sum_{r=1}^{|A_j^0 \setminus B_j^0|} \mathbf{q}_{jr} \mathbf{q}_{jr}^\top$. Let $\mathbf{Q}_j = (\mathbf{q}_{j1}, \dots, \mathbf{q}_{j, |A_j^0 \setminus B_j^0|}) \in \mathbb{R}^{n \times |A_j^0 \setminus B_j^0|}$. Then

$$\begin{pmatrix} \mathbf{Q}_j^\top \mathbf{e}_j \\ \boldsymbol{\eta}_j \end{pmatrix} \Bigg| \mathbb{Y}_{\text{AN}(j)}, \mathbb{X} \sim N \left(\mathbf{0}, \begin{pmatrix} \mathbf{I}_{|A_j^0 \setminus B_j^0|} & n^{-1/2} \mathbf{Q}_j^\top \mathbb{Y}_{A_j^0 \setminus B_j^0} \\ n^{-1/2} \mathbb{Y}_{A_j^0 \setminus B_j^0}^\top \mathbf{Q}_j & n^{-1} \mathbb{Y}_{A_j^0 \setminus B_j^0}^\top \mathbb{Y}_{A_j^0 \setminus B_j^0} \end{pmatrix} \right),$$

and hence, $\mathbf{Q}_j^\top \mathbf{e}_j \mid \boldsymbol{\eta}_j, \mathbb{Y}_{\text{AN}(j)}, \mathbb{X} \sim N\left(n^{-1/2} \mathbb{Y}_{A_j^0 \setminus B_j^0}^\top \mathbf{Q}_j \boldsymbol{\eta}_j, \mathbb{Y}_{A_j^0 \setminus B_j^0}^\top (\mathbf{I}_n - \mathbf{Q}_j \mathbf{Q}_j^\top) \mathbb{Y}_{A_j^0 \setminus B_j^0}\right)$. Next, let j^* be a leaf node of the graph \mathcal{G}^0 . For fixed $|D| > 0$, after change of measure,

$$\begin{aligned} \beta(\boldsymbol{\theta}^0, \mathbf{H}) &\geq \liminf_{n \rightarrow \infty} E_{\boldsymbol{\theta}^0} \left(I \left(\sum_{j=1}^p \|\mathbf{Q}_j^\top \mathbf{e}_j\|_2^2 > \chi_{|D|, 1-\alpha}^2 \right) \exp(l(\boldsymbol{\theta}^n) - l(\boldsymbol{\theta}^0)) \right) \\ &= \liminf_{n \rightarrow \infty} E_{\boldsymbol{\theta}^0} E \left(I \left(\sum_{j=1}^p \|\mathbf{Q}_j^\top \mathbf{e}_j\|_2^2 > \chi_{|D|, 1-\alpha}^2 \right) \exp(l(\boldsymbol{\theta}^n) - l(\boldsymbol{\theta}^0)) \mid \mathbb{Y}_{-j^*} \mathbb{X} \right) \\ &= \liminf_{n \rightarrow \infty} E \left(P \left(\|\mathbf{Z}_{j^*} + \mathbf{Q}_{j^*}^\top \mathbb{Y}_{A_{j^*}^0 \setminus B_{j^*}^0} \boldsymbol{\Delta}_{j^*}\|_2^2 + \sum_{j \neq j^*} \|\mathbf{Q}_j^\top \mathbf{e}_j\|_2^2 > \chi_{|D|, 1-\alpha}^2 \mid \mathbb{Y}_{-j^*}, \mathbb{X} \right) \right), \end{aligned}$$

where $\mathbf{Z}_{j^*} \sim N(\mathbf{0}, \mathbf{I}_{|A_{j^*}^0 \setminus B_{j^*}^0|})$. Note that $\|\mathbf{Q}_{j^*}^\top \mathbb{Y}_{A_{j^*}^0 \setminus B_{j^*}^0} \boldsymbol{\Delta}_{j^*}\|_2^2 \geq c_3 \|\boldsymbol{\Delta}_{j^*}\|_2^2$ with probability tending to 1 (Lemma 3 of (Li et al., 2019)). Therefore, the peeling process yields $\beta(\boldsymbol{\theta}^0, \mathbf{H}) \geq P(\|\mathbf{Z} + c_3 \mathbf{H}\|_2^2 \geq \chi_{|D|, 1-\alpha}^2)$, where $\mathbf{Z} \sim N(\mathbf{0}, \mathbf{I}_{|D|})$. Similarly, as $|D| \rightarrow \infty$,

$$\beta(\boldsymbol{\theta}^0, \mathbf{H}) \geq P\left(\|\mathbf{Z} + c_3 \mathbf{H}\|_2^2 > (2|D|)^{1/2} z_{1-\alpha} + |D|\right) \rightarrow P\left(Z > z_{1-\alpha} - c_3 \|\mathbf{H}\|_2^2 / \sqrt{2|D|}\right).$$

This completes the proof.

Proof of Proposition 7

By Proposition 6, for fixed $|D| = |F| > 0$, $\beta(\boldsymbol{\theta}^0, \mathbf{H})$ equals to

$$P(\text{Pval}_1 < \alpha, \dots, \text{Pval}_{|F|} < \alpha) \geq 1 - \sum_{k=1}^{|F|} P(\text{Pval}_k \leq \alpha) \geq 1 - |F| P(Z_1^2 \leq \chi_{1, 1-\alpha}^2),$$

where $Z_1 \sim N(h / \max_{j=1}^p \Omega_{jj}, 1)$. Then $P(\tilde{Z}^2 \leq x) \leq P(\tilde{Z} \leq -\mu + \sqrt{x}) \leq \frac{1}{\sqrt{2\pi}} \frac{e^{-(\mu - \sqrt{x})^2/2}}{\mu - \sqrt{x}}$ for $\tilde{Z} \sim N(\mu, 1)$ and any $0 \leq x < \mu^2$ and $\mu > 0$ (Small, 2010). Hence, as $|D| = |F| \rightarrow \infty$,

$$\beta(\boldsymbol{\theta}^0, \mathbf{H}) \geq 1 - |F| P(Z_1^2 \leq \chi_{1, 1-\alpha}^2) \geq 1 - \frac{|F|}{\sqrt{2\pi}} e^{-(h\sqrt{\log |F|} / \max_{j=1}^p \Omega_{jj} - \sqrt{\chi_{1, 1-\alpha}^2})^2/2} \rightarrow 1.$$

This completes the proof.

References

- B. Aragam, A. Amini, and Q. Zhou. Globally optimal score-based learning of directed acyclic graphs in high-dimensions. In *Advances in Neural Information Processing Systems*, pages 4452–4464, 2019.
- P. J. Bickel, Y. Ritov, A. B. Tsybakov, et al. Simultaneous analysis of lasso and dantzig selector. *The Annals of Statistics*, 37(4):1705–1732, 2009.

- L. Breiman. The little bootstrap and other methods for dimensionality selection in regression: X-fixed prediction error. *Journal of the American Statistical Association*, 87(419):738–754, 1992.
- C. Chen, M. Ren, M. Zhang, and D. Zhang. A two-stage penalized least squares method for constructing large systems of structural equations. *The Journal of Machine Learning Research*, 19(1):40–73, 2018.
- D. M. Chickering. Optimal structure identification with greedy search. *The Journal of Machine Learning Research*, 3:507–554, 2003.
- D. Eaton and K. Murphy. Exact bayesian structure learning from uncertain interventions. In *Artificial intelligence and statistics*, pages 107–114, 2007.
- B. Efron, T. Hastie, I. Johnstone, R. Tibshirani, et al. Least angle regression. *The Annals of statistics*, 32(2):407–499, 2004.
- J. Fan, L. Xue, H. Zou, et al. Strong oracle optimality of folded concave penalized estimation. *The Annals of Statistics*, 42(3):819–849, 2014.
- N. Friedman and D. Koller. Being bayesian about network structure. a bayesian approach to structure discovery in bayesian networks. *Machine learning*, 50(1-2):95–125, 2003.
- F. G. Gervais, D. Xu, G. S. Robertson, J. P. Vaillancourt, Y. Zhu, J. Huang, A. LeBlanc, D. Smith, M. Rigby, M. S. Shearman, et al. Involvement of caspases in proteolytic cleavage of alzheimer’s amyloid- β precursor protein and amyloidogenic $a\beta$ peptide formation. *Cell*, 97(3):395–406, 1999.
- A. Goate, M.-C. Chartier-Harlin, M. Mullan, J. Brown, F. Crawford, L. Fidani, L. Giuffra, A. Haynes, N. Irving, L. James, et al. Segregation of a missense mutation in the amyloid precursor protein gene with familial alzheimer’s disease. *Nature*, 349(6311):704–706, 1991.
- C. Heinze-Deml, M. H. Maathuis, and N. Meinshausen. Causal structure learning. *Annual Review of Statistics and Its Application*, 5:371–391, 2018.
- P. O. Hoyer, D. Janzing, J. M. Mooij, J. Peters, and B. Schölkopf. Nonlinear causal discovery with additive noise models. In *Advances in neural information processing systems*, pages 689–696, 2009.
- A. L. Jackson, S. R. Bartz, J. Schelter, S. V. Kobayashi, J. Burchard, M. Mao, B. Li, G. Cavet, and P. S. Linsley. Expression profiling reveals off-target gene regulation by rnaï. *Nature biotechnology*, 21(6):635–637, 2003.
- J. Janková and S. van de Geer. Inference in high-dimensional graphical models. *arXiv preprint arXiv:1801.08512*, 2018.
- M. Kanehisa and S. Goto. Kegg: kyoto encyclopedia of genes and genomes. *Nucleic acids research*, 28(1):27–30, 2000.
- A. Kleiner, A. Talwalkar, P. Sarkar, and M. Jordan. The big data bootstrap. *arXiv preprint arXiv:1206.6415*, 2012.

- M. M. Kulkarni, M. Booker, S. J. Silver, A. Friedman, P. Hong, N. Perrimon, and B. Mathey-Prevot. Evidence of off-target effects associated with long dsrnas in drosophila melanogaster cell-based assays. *Nature methods*, 3(10):833–838, 2006.
- B. Laurent and P. Massart. Adaptive estimation of a quadratic functional by model selection. *Annals of Statistics*, pages 1302–1338, 2000.
- C. Li, X. Shen, and W. Pan. Likelihood ratio tests for a large directed acyclic graph. *Journal of the American Statistical Association*, pages 1–16, 2019.
- Z. Liu, M. Zhang, G. Xu, C. Huo, Q. Tan, Z. Li, and Q. Yuan. Effective connectivity analysis of the brain network in drivers during actual driving using near-infrared spectroscopy. *Frontiers in behavioral neuroscience*, 11:211, 2017.
- P.-L. Loh, M. J. Wainwright, et al. Support recovery without incoherence: A case for nonconvex regularization. *The Annals of Statistics*, 45(6):2455–2482, 2017.
- R. Luo and H. Zhao. Bayesian hierarchical modeling for signaling pathway inference from single cell interventional data. *The Annals of Applied Statistics*, 5(2A):725, 2011.
- A. J. Molstad, W. Sun, and L. Hsu. A covariance-enhanced approach to multitissue joint eqtl mapping with application to transcriptome-wide association studies. *The Annals of Applied Statistics*, 15(2):998–1016, 2021.
- C. J. Oates, J. Q. Smith, and S. Mukherjee. Estimating causal structure using conditional dag models. *The Journal of Machine Learning Research*, 17(1):1880–1903, 2016.
- J. Pearl. *Causality: models, reasoning and inference*. Cambridge Univ Press, 2000.
- J. Peters and P. Bühlmann. Identifiability of gaussian structural equation models with equal error variances. *Biometrika*, 101(1):219–228, 2014.
- J. Peters, P. Bühlmann, and N. Meinshausen. Causal inference by using invariant prediction: identification and confidence intervals. *Journal of the Royal Statistical Society: Series B (Statistical Methodology)*, 78(5):947–1012, 2016.
- D. Rothenhäusler, P. Bühlmann, N. Meinshausen, et al. Causal dantzig: fast inference in linear structural equation models with hidden variables under additive interventions. *The Annals of Statistics*, 47(3):1688–1722, 2019.
- M. Rudelson and S. Zhou. Reconstruction from anisotropic random measurements. In *Conference on Learning Theory*, pages 10–1, 2012.
- K. Sachs, O. Perez, D. Pe’er, D. A. Lauffenburger, and G. P. Nolan. Causal protein-signaling networks derived from multiparameter single-cell data. *Science*, 308(5721):523–529, 2005.
- X. Shen and J. Ye. Adaptive model selection. *Journal of the American Statistical Association*, 97(457):210–221, 2002.
- X. Shen, W. Pan, and Y. Zhu. Likelihood-based selection and sharp parameter estimation. *Journal of the American Statistical Association*, 107(497):223–232, 2012.

- X. Shen, W. Pan, Y. Zhu, and H. Zhou. On constrained and regularized high-dimensional regression. *Annals of the Institute of Statistical Mathematics*, 65(5):807–832, 2013.
- S. Shimizu, P. O. Hoyer, A. Hyvärinen, and A. Kerminen. A linear non-gaussian acyclic model for causal discovery. *Journal of Machine Learning Research*, 7(Oct):2003–2030, 2006.
- A. Shojaie and G. Michailidis. Penalized likelihood methods for estimation of sparse high-dimensional directed acyclic graphs. *Biometrika*, 97(3):519–538, 2010.
- C. G. Small. *Expansions and asymptotics for statistics*. Chapman and Hall/CRC, 2010.
- P. Spirtes, C. Glymour, and R. Scheines. *Causation, prediction, and search*. The MIT Press, 2000.
- C. Squires, Y. Wang, and C. Uhler. Permutation-based causal structure learning with unknown intervention targets. In *Conference on Uncertainty in Artificial Intelligence*, pages 1039–1048. PMLR, 2020.
- P. D. Tao et al. The dc (difference of convex functions) programming and dca revisited with dc models of real world nonconvex optimization problems. *Annals of operations research*, 133(1-4):23–46, 2005.
- A. Teumer. Common methods for performing mendelian randomization. *Frontiers in cardiovascular medicine*, 5:51, 2018.
- C. Uhler, G. Raskutti, P. Bühlmann, and B. Yu. Geometry of the faithfulness assumption in causal inference. *The Annals of Statistics*, 41(2):436–463, 2013.
- S. van de Geer and P. Bühlmann. l_0 -penalized maximum likelihood for sparse directed acyclic graphs. *The Annals of Statistics*, 41(2):536–567, 2013.
- F. Vanleuven. Gsk3 and alzheimer’s disease: facts and fictions. *Frontiers in molecular neuroscience*, 4:17, 2011.
- J. Viinikka, A. Hyttinen, J. Pensar, and M. Koivisto. Towards scalable bayesian learning of causal dags. *arXiv preprint arXiv:2010.00684*, 2020.
- Y. Yuan, X. Shen, W. Pan, and Z. Wang. Constrained likelihood for reconstructing a directed acyclic gaussian graph. *Biometrika*, 106:109–125, 2019.
- Y. Zhang, M. J. Wainwright, and M. I. Jordan. Lower bounds on the performance of polynomial-time algorithms for sparse linear regression. In *Conference on Learning Theory*, pages 921–948, 2014.
- T. Zhao, H. Liu, T. Zhang, et al. Pathwise coordinate optimization for sparse learning: Algorithm and theory. *The Annals of Statistics*, 46(1):180–218, 2018.
- X. Zheng, B. Aragam, P. K. Ravikumar, and E. P. Xing. Dags with no tears: Continuous optimization for structure learning. In *Advances in Neural Information Processing Systems*, pages 9472–9483, 2018.

Y. Zhou, P. X.-K. Song, and X. Wen. Structural factor equation models for causal network construction via directed acyclic mixed graphs. *Biometrics*, 2021.